Indexing recruitment for source populations contributing to mixed fisheries by incorporating age in genetic stock identification models

Travis O. Brenden[1,2], Iyob Tsehaye[1,2], James R. Bence[1,2], Jeannette Kanefsky[2], and Kim T. Scribner[2]

[1] *Quantitative Fisheries Center, Michigan State University, 375 Wilson Road, East Lansing, Michigan 48824, USA*

[2] *Department of Fisheries and Wildlife, Michigan State University, 480 Wilson Rd., East Lansing, Michigan 48824, USA*

Abstract: We describe a methodology for estimating relative recruitments for source populations (sources) contributing to mixed fisheries by incorporating age into genetic stock identification models. The approach produced recruitment estimates that were strongly correlated (median correlation = 0.849; 2.5 and 97.5 percentile in correlations = 0.613 and 0.951) with simulated recruitments across various design factors, including number of sources, genetic divergence among sources, and temporal variation in source recruitments. Sensitivity analyses indicated that the approach was robust to aging inaccuracies and assumed source mortalities. Application to walleye *Sander vitreus* sources contributing to the Saginaw Bay, Lake Huron fishery produced similar recruitment estimates to assessment models. There was greater discrepancy between recruitment estimates for lake trout *Salvelinus namaycush* hatchery strains in northern Lake Michigan when compared to strain stocking levels, although this mismatch may stem from stocking levels being a poor recruitment measure. The estimation approach should prove beneficial for indexing source recruitment based on fishery or assessment collections from mixtures, even when long-term time-series of harvest and survey data required for integrated assessments are not available.

Introduction

Recruitment (number of hatched individuals surviving early-life mortality) is one of the fundamental rate functions governing the dynamics of populations, along with growth and mortality of older individuals. Often in marine and freshwater fish populations, recruitment is characterized by considerable spatial and temporal variation (Sissenwine 1984; Fogarty 1993; Myers et al. 1997; Thorson et al. 2014; Hansen et al. 2015). Recruitment levels can vary in response to spawning stock size due to associated changes in the number and quality of progeny produced, and density-dependent early life survival, and the influence of these factors are reflected in stock-recruitment models. Although there are cases where average recruitment stays nearly constant over a range of stock sizes (e.g., when the stock-recruitment relationship is steep and approaches an asymptote), recruitment levels still typically vary substantially due to biological, physical, and environmental factors that influence early-life survival, spawning stock fecundity, or other aspects of the regeneration cycle of populations (Hilborn and Walters 1992; Quinn and Deriso 1999).

From a fisheries management perspective, knowledge of recruitment patterns, underlying relationships with spawning stock biomass, and the extent of variability within and among populations is considered critical (Miller 2007; Ludsin et al. 2014). The relationship between spawning stock biomass and subsequent reproduction and recruitment to the fishable population largely dictate how much yield can be sustainably harvested from populations, which has resulted in the identification and wide use of harvest policies based on reference points derived from review of stock-recruitment relationships for fish stocks (Mace 1994; Myers et al. 1994). In cases of mixed fisheries [i.e., fisheries that exploit individuals from multiple source populations (hereafter mixtures)], an understanding of recruitment levels and variability in recruitment of

55 individual source populations is also important as less productive populations can be
56 overharvested if policies do not account for productivity differences among populations
57 (Hutchings 1996, 2000; Stephenson 1999; Frank and Brickman 2000; Reiss et al. 2009).
58 Unfortunately, accurate evaluation of recruitment levels of source populations (hereafter sources)
59 that contribute to mixtures can be difficult if assessment sampling is not conducted when
60 populations are separated (Guan et al. 2013; Li et al. 2015).

61 Herein, we propose a methodological approach for estimating annual relative recruitment
62 levels for sources based on recreational, commercial, or assessment collections from mixtures,
63 and use simulations to evaluate the estimation performance of the approach. The proposed
64 methodology incorporates age of fish collected from mixtures into widely used model-based
65 genetic stock identification (GSI) analyses (e.g., Pella and Milner 1987; Pella and Masuda 2001).
66 Bjorndal and Bolten (2008) previously noted that temporal variation in source contributions to
67 mixtures can arise from variations in recruitment, mortality, and/or emigration. The methodology
68 we propose is premised on using observed temporal variability in source contributions and
69 available information on mortality and limiting assumptions on movement as a means to index
70 annual changes in source-specific recruitment levels. Whereas similar approaches have assumed
71 that annual changes in recruitment levels of sources are consistent across years (Tsehaye et al.
72 2016), the approach we present here allows for annual fluctuations in source recruitment levels.
73 The availability of genetic data is increasing, as is the awareness of how these data can be used
74 in stock assessments (Spies and Punt 2015). We emphasize that our proposed methodology has
75 more limited objectives (estimation of relative recruitment from multiple sources to a mixture)
76 and substantially lower data requirements than a spatially explicit integrated assessment would.

We provide two empirical applications of the proposed methodology using mixture data for walleye *Sander vitreus* from Saginaw Bay, Lake Huron and lake trout *Salvelinus namaycush* from northern Lake Michigan. For the walleye example, the contributing sources were Lake Huron and Lakes Erie and St. Clair (hereafter Lake Erie/St. Clair) walleye populations (Fig. 1). For the lake trout example, the contributing source data consisted of different hatchery strains that have been stocked into Lake Michigan (i.e., until recently negligible wild reproduction of lake trout occurred in the lake) (Fig. 1). For both the walleye and lake trout examples, other estimates of recruitment levels for contributing sources were available to which recruitment estimates from our proposed methodology could be compared. The comparison of recruitment estimates from our proposed approach with those from these other data sources did not represent a true validation of the proposed methodology, as actual recruitment levels for both the walleye and lake trout case studies were unknown. However, the simulations that were conducted as part of this research did provide a means to validate performance accuracy, as in these cases recruitment levels of the sources were known.

Methods

Estimation approach

For regular model-based GSI analysis, the probability (π) of observing genotype samples (X) in a mixture given estimates of the source proportional contributions ($\boldsymbol{p}$) and allele relative frequencies at each locus and source ($\boldsymbol{Q}$) is generally specified as

$$\pi(\mathrm{X}|\boldsymbol{Q},\boldsymbol{p}) = \prod_{m=1}^{M}\sum_{i=1}^{I} p_i f\left(\mathrm{X}_m|\boldsymbol{Q}_i\right) \quad (1)$$

where M (m=1…M) is the number of fish sampled from the mixture, I (i=1…I) is the number of sources, p_i is the proportional contribution for the i-th source (i.e., the i-th element of $\boldsymbol{p}$) to the mixture, and $f(\mathrm{X}_m \mid \boldsymbol{Q}_i)$ is the probability of an individual from the i-th source having the same genotype as the m-th individual from the mixture, which is determined from the allele relative frequencies for the i-th source under an assumed genetic model (e.g., Hardy-Weinberg equilibrium) (Pella and Milner 1987; Pella and Masuda 2001). As in Pella and Masuda (2001), if $x_{m,h,j}$ denotes the count of the j-th allele of the h-th locus for the m-th individual, then X_m constitutes the collective allele counts for all loci for the m-th individual. As noted by Tsehaye et al. (2016), to infer changes in recruitment levels within the context of GSI analyses, proportional contributions for sources must be expanded to include ages of individuals collected from the mixture and when the mixture was sampled (i.e., sampling year). Thus, Equation 1 gets expanded to

$$\pi(\mathrm{X} \mid \boldsymbol{Q}, \boldsymbol{P}^s) = \prod_{m=1}^{M} \sum_{i=1}^{I} P_{i,a}^{s} f(\mathrm{X}_m \mid \boldsymbol{Q}_i) \qquad (2)$$

where X_m now also include the age (a) of the m-th individual along with the individual's multilocus genotype, $P_{i,a}^{s}$ is the proportional contribution of the i-th source population for the a-th age class in the s-th sampling year, and $\boldsymbol{P}^s$ is the collection of proportional contributions for the sources and age classes for a particular sampling year. As with $\boldsymbol{p}$, the elements of $\boldsymbol{P}^s$ for each sampling year are defined on the simplex (contributions must be greater than 0, less than 1, and must sum to 1 across all elements).

For indexing recruitment, Tsehaye et al. (2016) proposed modeling the elements of $\boldsymbol{P}^s$ through mathematical representation of the underlying population-specific processes affecting abundance levels. The population-specific process assumed by Tsehaye et al. (2016) was

intended for a long-lived species such as lake sturgeon *Acipenser fulvescens* with high pre-recruitment mortality and low (and relatively constant) post-recruitment mortality rates, which results in a constant rate of change in recruitment levels (on a $\log_e$ scale time) over time. We adopt a similar approach herein; however, we assume an underlying process that allows annual recruitment levels to fluctuate. Specifically, we propose that recruitment of the sources be modeled as multiplicative deviations from an overall grand mean recruitment level

$$N_{i,0}^{y} = \mu \cdot \exp\left(\tau_i + \gamma_y + \upsilon_{i,y}\right) \quad (3)$$

where $N_{i,0}^{y}$ is the abundance at age 0 (or an alternative specified age of recruitment) for the *i*-th source and the *y*-th year class, μ is the grand mean abundance at age of recruitment, τ_i are source deviations from the grand mean, γ_y are year-class deviations (i.e., coherent temporal deviations common to all sources) from the grand mean, and $\upsilon_{i,y}$ are source × year-class interaction deviations (i.e., ephemeral-temporal deviations that are independent year-class deviations for each source). Estimation of the grand mean abundance is generally not possible from mixture compositions. Consequently, Equation 3 reduces to

$$\log_e(\widetilde{N}_{i,0}^{y}) = \tau_i + \gamma_y + \upsilon_{i,y} \quad (4)$$

where $\widetilde{N}_{i,0}^{y}$ is the relative recruitment levels for the sources (i.e. $\widetilde{N}_{i,0}^{y} = N_{i,0}^{y} / \mu$).

Relative abundances at age for the sources associated with different year classes can be forward projected using a standard exponential mortality model

$$\log_e(\widetilde{N}_{i,a}^{y}) = \log_e(\widetilde{N}_{i,0}^{y}) - \sum_{o=1}^{a} Z_{i,o-1} \quad (5)$$

where $\sum_{o=1}^{a} Z_{i,o-1}$ is the cumulative instantaneous total mortality experienced by the *i*-th source up to the *a*-th age and *o* is used to index age. With a mixture fishery operating in a specific location

141 of a system, only certain fractions of the sources are likely to move to this region and be subject
142 to exploitation. Thus, the expected relative abundances at age for the sources located within the
143 boundaries where a mixed fishery operates is

144 $$\ddot{N}_{i,a}^{y} = d_{i,a}\tilde{N}_{i,a}^{y} \quad (6)$$

145 where $d_{i,a}$ is the fraction of fish from the *i*-th source and *a*-th age that move into the region of
146 the mixture fishery.

147 When collections are made from mixtures in a particular sampling year, collected
148 individuals represent a range of year classes with the range depending on the sampling year and
149 ages of collected individuals. Consequently, the expected proportional contributions to a mixture
150 from the *i*-th source for the *a*-th age can be calculated as

151 $$P_{i,a}^{s} = \frac{\ddot{N}_{i,a}^{s-a}}{\sum_{i=1}^{I}\sum_{o=\min(\text{age})}^{\max(\text{age})}\ddot{N}_{i,o}^{s-o}} \quad (7)$$

152 where min(age) and max(age) indicate the minimum and maximum age, respectively, in the
153 mixture and *s*-*o* and *s*-*a* indexes the correct year class for calculating the contributions. As
154 previously indicated, temporal variations in source contributions to mixtures can arise from
155 variations in recruitment, mortality, and/or emigration (Bjorndal and Bolten 2008), and this is
156 evident from Equations 5-7. This means that relative recruitment levels, total mortalities, and
157 movement rates are confounded, thus simplifications and/or assumptions must be made to assess
158 recruitment based on mixture compositions. For our application, we assume that age-specific
159 total mortality estimates for the sources will be available based on other types of analyses, such
160 as catch curve assessments, tagging studies, or other types of direct or indirect methods (Ricker
161 1975; Hewitt et al. 2007; Then et al. 2014). With respect to movement, it is not necessary for
162 actual movement rates to be known for the sources and ages for recruitment to be indexed based

on the above approach. Rather, it is only necessary for movement rates to be constant across ages within a source for using the approach to index inter-annual variation in relative recruitments. If estimates of source-specific movement rates to the mixture are available, then relative recruitment comparisons across sources can be made so long as source vulnerability to assessment or fishing gear in the mixture is the same.

Under this formulation, the probability in equation 2 can be re-expressed as

$$\pi(\mathrm{X} \mid \boldsymbol{Q}, \boldsymbol{\tau}, \boldsymbol{\gamma}, \boldsymbol{\upsilon}) = \prod_{m=1}^{M} \sum_{i=1}^{I} \left(P_{i,a}^{s}(\boldsymbol{\tau}, \boldsymbol{\gamma}, \boldsymbol{\upsilon})\right) f\left(\mathrm{X}_{m} \mid \boldsymbol{Q}_{i}\right) \quad (8)$$

where $P_{i,a}^{s}(\boldsymbol{\tau}, \boldsymbol{\gamma}, \boldsymbol{\upsilon})$ is used to denote that $P_{i,a}^{s}$ is a function of $\boldsymbol{\tau}, \boldsymbol{\gamma}$, and $\boldsymbol{\upsilon}$. We do not include total mortality and movement rates in the function for $P_{i,a}^{s}$ as in our application we are treating these as fixed constants rather than parameters to be estimated. Equation 8 assumes that ages of individuals from the mixture can be accurately assigned. When aging error occurs, however, the uncertainty in age estimates can be incorporated in the probability calculations as this uncertainty can influence recruitment parameter estimates. With the incorporation of aging error, the probability in Equation 8 gets expanded to

$$\pi(\mathrm{X} \mid \boldsymbol{Q}, \boldsymbol{\tau}, \boldsymbol{\gamma}, \boldsymbol{\upsilon}) = \prod_{m=1}^{M} \sum_{i=1}^{I} \sum_{b=\min(\mathrm{age})}^{\max(\mathrm{age})} T(a \mid b)\left(P_{i,a}^{s}(\boldsymbol{\tau}, \boldsymbol{\gamma}, \boldsymbol{\upsilon})\right) f\left(\mathrm{X}_{m} \mid \boldsymbol{Q}_{i}\right) \quad (9)$$

where $T(a \mid b)$ is the probability that an individual identified as being age a is actually age b. Equation 9 does not include parameters associated with calculating the aging error matrix because for simplicity we treat these as known values. In principle, we could include the data needed to estimate the aging error, and estimate parameters needed to construct the matrix in conjunction with the recruitment change parameters, which would necessitate modification to Equation 9.

We programmed the estimation approach described above in AD Model Builder (Fournier et al. 2012). In previous work (Brenden et al. 2015a), we found that accuracy and precision of source contribution estimates to mixture fisheries derived from AD Model Builder were similar to estimates obtained from other routinely used estimation packages for GSI analyses. When estimating $\boldsymbol{\tau}$, $\boldsymbol{\gamma}$, and $\boldsymbol{\upsilon}$, we imposed the constraint that the sums of the elements of each must equal 0. Without these constraints, solutions to $\boldsymbol{\tau}$ and $\boldsymbol{\gamma}$ were not unique and different values could produce the exact same $\boldsymbol{P}^s$ given equation 7. The constraint on $\boldsymbol{\upsilon}$ was not necessary to produce unique parameter estimates but it reduced the number of estimated parameters and therefore affected measures of uncertainty of point estimates while having no real consequence on resulting relative recruitment estimates.

Under a Bayesian estimation approach, the posterior probability distributions for the unknown parameters can be specified as

$$\pi(\boldsymbol{Q},\boldsymbol{\tau},\boldsymbol{\gamma},\boldsymbol{\upsilon}\,|\,\mathrm{X},\mathrm{Y}) \propto \pi(\mathrm{X}\,|\,\boldsymbol{Q},\boldsymbol{\tau},\boldsymbol{\gamma},\boldsymbol{\upsilon})\pi(\boldsymbol{Q}\,|\,\mathrm{Y})\pi(\boldsymbol{\tau})\pi(\boldsymbol{\gamma})\pi(\boldsymbol{\upsilon}), \quad (10)$$

where $\pi(\boldsymbol{\tau})$, $\pi(\boldsymbol{\gamma})$, and $\pi(\boldsymbol{\upsilon})$ are the prior probability distributions assigned to the parameters describing changes in relative recruitment levels, $\pi(\mathbf{Q}\,|\,\mathrm{Y})$ is the prior probability distribution for allele relative frequencies of the baseline populations ($\boldsymbol{Q}$) given the collection and genotyping of individuals from the baseline populations (Y), and $\pi(\mathrm{X}\,|\,\boldsymbol{Q},\boldsymbol{\tau},\boldsymbol{\gamma},\boldsymbol{\upsilon})$ is as defined in equations 9 or 10 depending on whether aging error occurs. Our specification of $\pi(\boldsymbol{Q}\,|\,\mathrm{Y})$ followed the multinomial-Dirichlet hyperparameter updating procedure described in Corander et al. (2006). For $\pi(\boldsymbol{\tau})$ and $\pi(\boldsymbol{\gamma})$, uniform distributions with lower and upper limits of -5.0 and +5.0, respectively, were assumed. The intent of the uniform prior distribution was to provide weakly informative priors so that estimates of $\boldsymbol{\tau}$ and $\boldsymbol{\gamma}$ would largely be influenced by the data, while ensuring a proper posterior distribution and avoiding individual effects getting stuck at extremely

high or low values. Given that these parameters influence relative recruitment on a logarithmic scale, the range of relative recruitments allowed by the uniform distribution is over 22,000 fold. For $\pi(\boldsymbol{\upsilon})$, a normal distribution with a mean of 0.0 and standard deviation of 3.0 was assumed. This too was intended to be weakly informative but with a tendency toward a zero estimate in the absence of other information. Thus, we treated the $\boldsymbol{\upsilon}$ as random effects from a shared stochastic process, with average levels (i.e., 0) being more likely than extreme ones. Preliminary evaluations suggested that with sufficiently large sample sizes from the mixture, the standard deviation for the normal prior distribution on $\pi(\boldsymbol{\upsilon})$ could be estimated as part of the model fitting process, but at smaller sample sizes models that attempted to estimate the standard deviation would not converge on a solution. We therefore elected to fix the standard deviation at a value (3.0) corresponding to a relatively uninformative prior distribution for $\boldsymbol{\upsilon}$.

Baseline simulations

Simulation factor levels.— Our simulation framework generated for a single simulation (1) expected genotype proportions by source and loci, (2) expected age compositions by source and sampling year, (3) observed genotype samples from the sources, and (4) observed genotype and age composition data from the mixture (Fig. 2, see Appendix A for technical details). Each individual simulation for a specific scenario was defined by specified inputs and produced different expected genotype proportions and different expected age compositions due to random factors such as number of loci, number of alleles for each locus, and temporal and spatial variation in recruitment, and given these expectations there was random variation in the resulting source and mixture data (Fig. 2). The estimation model was then applied to each set of simulated data (Fig. 2).

We used the simulation model to generate source and mixture observations under a range of conditions, including two numbers of sources (6 or 12 populations), three levels of genetic divergence (θ) among sources (0.01, 0.06, or varied [$\theta_{High} = 0.051$, $\theta_{Low} = 0.01$], two levels of difference in the source effects (low or high), three levels of total temporal variation in (0.7, 1.0., or 2.0) (see Appendix A), three variation ratios (1:4, 1:1, 4:1) dictating how total temporal recruitment variation was allocated between the two sources of variation (e.g., 1:4 means 20% of total temporal variation was allocated to year-class variation and 80% was allocated to source × year-class variation), two levels of sampling duration (two or six years), and three mixture sample sizes (100, 300, or 500 fish per year). Under a low difference in source effects, the source-specific deviations (τ_i) were set such that the largest difference in expected recruitment between any two sources contributing to the mixture would be 10-fold (i.e., $\exp(\max(\boldsymbol{\tau}))/\exp(\min(\boldsymbol{\tau})) = 10$) (Table 1). Under a high difference in source effects, the τ_i values were set such that the largest difference in expected recruitment between any two sources contributing to the mixture would be 40-fold (i.e., $\exp(\max(\boldsymbol{\tau}))/\exp(\min(\boldsymbol{\tau})) = 40$) (Table 1).

We used a full factorial design so that all 648 combinations of factors levels were evaluated, with 1,000 simulations conducted for each factor-level combination. For all simulations, we assumed sample sizes of 200 fish per source for the calculations of allele relative frequencies, age 2 was the age of recruitment with ages of individuals collected from the mixture ranging from age 2 to age 9, and that there was no aging error. Previous research found the source sample sizes ranging from 50 to 200 fish per source explained very little of the variability in genetic stock identification results (Brenden et al. 2015a), which was why we did not explore varying source sample sizes. The age range assumed in the simulations was arbitrary but was mid-range to the age ranges incorporated in stock assessment models used for managing lake

253 trout, walleye, Chinook salmon (*Oncorhynchus tshawytscha)* and lake whitefish (*Coregonus*
254 *clupeaformis*) populations in the Great Lakes (Brenden et al. 2011; Berger et al. 2012; Brenden
255 et al. 2012; Fielder and Bence 2014; Tsehaye et al. 2014). For each simulation, the number of
256 loci used to genotype source and mixture fish was randomly selected from between 10 and 30
257 loci. Similarly, the number of alleles was randomly selected for each locus and simulation and
258 could range from 5 to 25 alleles.

259 Models were fit by highest posterior density estimation, meaning that Markov Chain
260 Monte Carlo (MCMC) procedures were not used to characterize the full posterior probability of
261 the parameters. Highest posterior density estimation is also referred to as penalized maximum
262 likelihood estimation. We chose to use this estimation approach because for the simulations a
263 total of 648,000 models were fit and thus it was time prohibitive to conduct a full Bayesian
264 estimation of the models. The objective function for the estimation models corresponded to the
265 sum of the negative $\log_e$ likelihood (i.e., negative $\log_e$ of Equation 8) and prior probability
266 distributions for the $\boldsymbol{\tau}$, $\boldsymbol{\gamma}$, and $\boldsymbol{\upsilon}$. As previously indicated, models were fit in AD Model Builder
267 (Fournier et al. 2012). Models were considered to have converged on a solution when the
268 maximum gradient of the parameters with respect to the objective function was less than 1.0E-3.
269
270 *Performance measures*.— For each simulation, we calculated the Pearson correlation between
271 estimated and true $\log_e$ relative recruitments across all sources. A multifactor ANOVA model
272 was fit to the correlations from the simulations to assess the importance of the investigated
273 factors. We used eta-squared (η^2) values to estimates of the amount of variability in correlations
274 accounted for by main effects and all main-effect interactions (i.e., up to seventh-order
275 interactions) (Corell et al. 2012). The median and interquartile range (IQR) of the correlations in

276 the recruitment values from across all simulations conducted for a particular combination of
277 factor levels were used as measures of accuracy and precision, respectively. Only factor level
278 combinations (e.g., main factors, second-order interactions) that were identified as being
279 important from the multifactor ANOVA η^2 values were used in summarizing results.
280
281 **Sensitivity analyses**
282 Sensitivity of the estimation approach to errors in total mortalities and aging uncertainty
283 was explored to assess robustness of the method. Based on the results of the baseline simulations
284 (see below), sensitivity analyses were conducted for the two source numbers (6 or 12 sources),
285 the three levels of genetic divergence among sources (0.01, 0.06, or varied), and three mixture
286 sample sizes (100, 300, or 500 fish). All sensitivity simulations assumed a two-year sampling
287 duration, a high difference in source population effect, a total temporal variation in recruitment
288 of 2.0, and a 4:1 ratio for how total temporal variation in recruitment was allocated between
289 year-class and source × year-class variation. As in the base simulations, we assumed sample
290 sizes of 200 fish per source, ages of individuals collected from the mixture ranging from age 2 to
291 age 9, the number of loci used to genotype source and mixture fish was randomly selected from
292 between 10 and 30 loci for each iteration, and the number of alleles was randomly selected for
293 each locus and iteration and could range from 5 to 25 alleles.
294 In terms of sensitivity to incorrect assumptions regarding total mortality, we considered
295 three different scenarios. In the first scenario (random mortality scenario), we randomly
296 generated total mortalities for each source, year-class, and age from normal distributions with a
297 mean of 0.30 and a standard deviation of 0.04 for simulation data. In the second scenario
298 (autocorrelated mortality scenario), age-specific deviations in total mortalities from an average

rate of 0.30 for each source and year-class were generated from a first-order autoregressive process [AR(1)]. Values from an AR(1) process with a mean of 0.0, autoregressive coefficient of 0.8, and innovations variance of 0.15 were generated, exponentiated, and multiplied by 0.30. In the third scenario (population mortality scenario), age-specific total mortalities for the sources were generated from normal distributions with means for the different sources ranging from 0.20 to 0.40 at equispaced intervals (0.04 interval for 6 sources; 0.0182 interval for 12 sources) and standard deviations of 0.04. For each mortality sensitivity scenario, we continued to assume source- and age-specific total mortalities of 0.30 in the estimation program, meaning that we assessed the consequences on estimation performance when assumed mortalities were different (and more simplistic) than the mortality rates actually experienced by the source populations.

For aging uncertainty, we generated an aging error matrix based on the method of Richards et al. (1992) whereby the distribution of estimated ages given expected true ages was modeled through discretized normal distributions. Expectations of estimated age given true age were modeled as a linear function of true age with an intercept of 0 and a slope of 1.0 (Richards et al. 1992). The standard deviation of estimated ages (σ_a) was modeled as a linear function of the expected true age with an intercept of 0 and a slope of 0.06 (low aging error) or 0.10 (high aging error). With a slope of 0.06, aging uncertainty ranged from 0% for younger ages to approximately 20% (i.e., 10% of individuals underestimated in age by and 10% overestimated in age) for older ages. With a slope of 0.10, aging uncertainty ranged from 0% for younger ages to approximately 50% (i.e., 25% of individuals underestimated in age and 25% of individuals overestimated in age) for older ages. Observed ages of mixture individuals were assigned by random sampling from multinomial distributions with probabilities equal to the age frequencies generated from the aging error matrix. For estimating recruitment levels under the aging

uncertainty sensitivity scenarios, we considered situations where aging was assumed to be accurate in the estimation model (i.e., $T(a \mid b)$ set equal to an identity matrix) and where the actual aging error matrix generated from the discretized normal distribution process described above was incorporated in the estimation model.

As part of the aging uncertainty analyses, we found that with high aging error the incorporation of the actual aging error matrix performed worse than when aging was assumed to be accurate (*see Sensitivity analyses results*). This was most noticeable at small sample sizes. To verify that this result was a sample size issue, we conducted additional sensitivity simulations with mixture sample sizes as large as 3000 fish per year for high aging error to determine whether with large enough sample sizes the incorporation of the actual aging error matrix would perform better than when aging was assumed to be accurate.

Empirical applications

For the empirical applications, we used a full Bayesian approach for model estimation so as to better characterize uncertainty in relative recruitments for the sources. Posterior probability distributions of the relative recruitments for each source and year-class combinations were characterized by MCMC simulations through a Metropolis-Hastings algorithm (Fournier et al. 2012). For the walleye application (described below), five independent MCMC chains were run for 500,000 steps sampling every 100th step, with the initial 2,500 saved steps discarded. For the lake trout application (described below), five independent MCMC chains were run for 5,000,000 steps sampling every 2,000th step, with the initial 500 saved steps discarded. Different chain lengths and sampling frequencies were necessary because the lake trout model was slower to converge and exhibited greater autocorrelation in the chain values. For both the walleye and lake

345 trout examples, one of the MCMC chains was initialized at the mode of the posterior probability
346 distributions for each parameter, whereas for the other four chains initialization values were
347 randomly generated from uniform distributions with lower and upper bounds of -5 and 5,
348 respectively, while imposing the zero-sum constraint on $\boldsymbol{\tau}, \boldsymbol{\gamma}$, and $\boldsymbol{\upsilon}$ as described in the *Estimation*
349 *approach* section. The random initialization values were generated in R (R Core Team 2014)
350 using the RandVec function in the "Surrogate" package (Van der Elst et al. 2017). Convergence
351 of each MCMC chain on stable distributions for all relative recruitments was evaluated
352 graphically with trace plots and analytically with Z-score tests to test differences between the
353 means of the first 10% and last 50% of the saved chains (Geweke 1992). Additionally, we
354 compared effective sample size of the saved MCMC chains with the actual chain sample sizes as
355 a method for evaluating autocorrelation among the saved samples. If each MCMC chain passed
356 the convergence diagnostics, convergence of the five MCMC chains on the same stationary
357 distribution was evaluated graphically by overlaying traceplots and analytically through potential
358 scale reduction factors (Gelman and Rubin 1992). The saved iterations from the five MCMC
359 chains were then combined and the median of the combined chains was used as the point
360 estimates for the relative recruitments. Uncertainty in the relative recruitments was based on the
361 95% highest posterior density intervals calculated across the combined MCMC chains. Similar
362 conclusions would have been reached if we had used highest posterior density estimates (i.e.,
363 mode of the posterior distributions) as point estimates for the relative recruitments. All MCMC
364 diagnostic measures were conducted in R using the "coda" package (Plummer et al. 2006).
365
366 *Saginaw Bay, Lake Huron Walleye*.—A description of the sampling and laboratory methods used
367 on the Saginaw Bay, Lake Huron walleye mixture and contributing sources is provided in

368 Brenden et al. (2015b). Briefly, fin-clip tissue samples were collected from seven source
369 populations located in Lakes Huron, St. Clair, and Erie. Multiple lines of evidence suggested
370 there was just two genetically distinct sources [Lake Huron source (represented by fish from the
371 Tittabawassee River) and a Lakes Erie/St. Clair source]. A total of 382 individuals from the
372 sources were genotyped for the determination of allele frequencies (Lake Huron: n=95; Lakes
373 Erie/St. Clair: n=287). Source tissue samples were genotyped at 10 microsatellite loci: *Svi*4,
374 *Svi*17, *Svi*18 and *Svi*33 (Borer et al. 1999); *Svi*L2, *Svi*L5, *Svi*L6 and *Svi*L8 (Wirth et al. 1999);
375 and *Svi*6 and *Svi*7 (Eldridge et al. 2002). Amplification conditions are described in Brenden et al.
376 (2015b), as are results pertaining to number of alleles, allelic richness, and observed and
377 expected heterozygosity.
378 Tissue samples from walleyes from the Saginaw Bay recreational fishery were collected
379 in 2008 and 2009 between the months of February and August. Ages of individuals collected
380 ranged from 3 to 15. For this study, we limited our analysis to walleye from the mixture that
381 were between age 3 and age 7 and that were collected between June to August. The oldest
382 walleye collected in 2008 was age 6 so based on available data we were able to index
383 recruitment for the 2002 to 2006 year classes. Tissue samples were available for a total of 262
384 individuals from the mixture (2008: n=138 fish; 2009: n=124 fish). We did not include walleye
385 collected between February and May as based on the results of Brenden et al. (2015b) there were
386 potential differences in migration rates between young and old walleye from the Lakes Erie/St.
387 Clair sources during these months, which would have influenced recruitment results. Mixture
388 tissue samples were genotyped using the same 10 microsatellite loci identified above for the
389 sources. Total instantaneous mortality rates for the corresponding year class and ages for the

sources were taken from Fielder and Bence (2014) and WTG (2014) and we assumed that aging error was negligible.

Estimated recruitment levels of the walleye source populations from our estimation approach for the 2002 to 2006 year classes were compared to corresponding recruitment estimates from SCAA models developed by Fielder and Bence (2014) for Lake Huron and WTG (2014) for Lake Erie. Comparisons between recruitment levels were based on Pearson correlations.

Northern Lake Michigan Lake trout.—As previously indicated, the source data for the lake trout empirical application consisted of different hatchery strains that have been stocked in Lake Michigan. An in-depth description of the hatchery source data and genotyping is provided in Appendix B. For these analyses, there were four hatchery strains for which there was sufficient information to distinguish among them. These hatchery strains were Lewis Lake, Seneca Lake, Green Lake, and Lake Superior. The Lake Superior hatchery strain was an aggregation of four separate hatchery strains derived from sources in Lake Superior (Isle Royale, Apostle Island, Marquette, Traverse Island) for which there was difficulty differentiating between given available data (Appendix B). A total of 669 individuals from the strains were genotyped for the determination of allele frequencies (Lewis Lake: n=98; Seneca Lake: n=101; Green Lake: n=100; Lake Superior: n=370). Hatchery strain tissue samples were genotyped at 10 microsatellite loci: *Sfo*1, *Sfo*12, and *Sfo*18 (Angers et al. 1995); *Scou*19 (Taylor et al. 2001); *One*μ9 and *One*μ10 (Scribner et al. 1996); *Ogo*1a (Olsen et al. 1998); *Ssa*85 (O'Reilly et al. 1996); and *Sfo*-C24 and *Sfo*-D75 (King et al. 2012).

412 The mixture samples for the lake trout application came from fin tissue samples collected
413 during fishery independent surveys and commercial fishery operations in the MM3 statistical
414 district in northern Lake Michigan (Fig. 2). Tissue sample were collected between the months of
415 April and September in 2009 and 2010. Mixture tissue samples were genotyped using the same
416 10 microsatellite loci identified above for the hatchery strains. We restricted our analyses to lake
417 trout ranging in age from 2 to 7. The oldest lake trout collected in 2009 was age 6 so based on
418 available data we were able to index recruitment for the 2003 to 2008 year classes. Ages were
419 assigned to lake trout through either scale readings or based on identifying fin clips (i.e., all lake
420 trout stocked in Lake Michigan in a given year are given a particular combination of fin clips).
421 Tissue samples were available for a total of 514 individuals from the mixture (2009: n=150 fish;
422 2010: n=364 fish). For this analysis, we assumed that lake trout aging error was negligible.
423 Age-specific mortality rates for the estimation model were taken from an SCAA model
424 that is used for setting allowable harvests in the management unit (Modeling Subcommittee,
425 Technical Fisheries Committee 2014). Past research has suggested that lake trout hatchery strains
426 may experience differential survival possibly as a consequence of strain-specific differences in
427 avoidance of sea lamprey *Petromyzon marinus* parasitism (Elrod et al. 1995, McKee et al. 2004).
428 While we do not discount the possibility of strain-specific differences in survival, strain-specific
429 estimates of mortality rates for lake trout in Lake Michigan were not available to incorporate in
430 this analysis.
431 Estimated recruitment levels of the lake trout hatchery strains from our estimation
432 approach was compared to the total number of lake trout stocked by hatchery strain for the
433 corresponding year classes we were able to index. The stocking information were from the Great
434 Lakes Fish Stocking Database (FWS/GLFC 2010). Although the lake trout mixture data were

435 from northern Lake Michigan, we considered stocking that occurred throughout Lake Michigan
436 given previous studies have found high dispersal rates of stock lake trout in the Great Lakes
437 (Adlerstein et al. 2007).
438

439 Results

440 **Baseline simulations**

441 The η^2 values obtained from the multifactor ANOVA model fit to the correlations
442 between estimated and true $\log_e$ relative recruitments indicated that main effects had the largest
443 influence on simulation results. The largest η^2 values for main effects were due to mixture
444 sample size ($\eta^2 = 23.6\%$), number of sources ($\eta^2 = 15.1\%$), and genetic divergence among the
445 source populations ($\eta^2 = 13.8\%$). Conversely, η^2 values were 6.0% for duration of sampling,
446 2.0% for level of difference in source effects, 1.3% for total temporal recruitment variation, and
447 1.1% for how total temporal recruitment variation was allocated between year-class and source ×
448 year-class variation. The largest η^2 values for second- or higher-order interactions among main
449 effects was 0.1%, with the vast majority of values being less than 0.01%, suggesting that
450 interactions among main effects were unimportant. Consequently, we chose to summarize
451 correlation results from the simulations only by main effect-factor levels.
452 Overall, the estimation approach performed well in estimating recruitment levels for the
453 sources. Across all simulations, the median correlation between estimated and true $\log_e$
454 recruitment levels for the sources was 0.849, with 2.5 and 97.5 percentile in correlations equal to
455 0.613 and 0.951, respectively. The correlation between estimated and true recruitment levels on a
456 non-logarithmic scale was even greater (median correlation=0.938; 2.5 and 97.5 percentile in

457 correlations equal to 0.659 and 0.994). As was expected, performance of the estimation approach
458 both with respect to accuracy and precision improved as mixture sample sizes and genetic
459 divergence among the sources increased. Median correlations in $\log_e$ recruitment levels were
460 0.788, 0.860, and 0.887 for mixture samples sizes of 100, 300, and 500 fish per year,
461 respectively, whereas IQR in correlations were 0.127, 0.093, and 0.080 for these same sample
462 sizes (Fig. 3). As genetic divergence among the sources increased from 0.01 to 0.06, median
463 correlations in $\log_e$ recruitment increased from 0.810 to 0.887, whereas IQR in correlations
464 decreased from 0.127 to 0.080 (Fig. 3). The varied genetic divergence level in which each source
465 had relatively low levels of genetic divergence with some of the sources and relatively high
466 levels of genetic divergence with the other sources had accuracy and precisions levels that were
467 intermediate of the results for 0.01 and 0.06 genetic divergences (Fig. 3).
468 As number of simulated sources increased, the accuracy and precision of the estimation
469 approach decreased (6 sources: median correlation = 0.882; IQR in correlations = 0.087; 12
470 sources: median correlation = 0.814; IQR in correlations = 0.118) (Fig. 3). Conversely, the
471 accuracy and precision of the estimation approach increased as sampling duration increased (2
472 year duration: median correlation = 0.828; IQR in correlations = 0.124; 6 year duration: median
473 correlation = 0.868; IQR in correlations = 0.097) (Fig. 3). Likewise, accuracy and precision
474 improved with increasing level of difference in source effects and total temporal variation in
475 recruitment. Median correlations in $\log_e$ recruitment were 0.835 and 0.863 and IQR in
476 correlations were 0.116 and 0.105 for low and high differences in source population effects,
477 respectively (Fig. 3). Median correlations in $\log_e$ recruitment were 0.839, 0.847, and 0.860 and
478 IQR in correlations were 0.122, 0.114, and 0.103 for total temporal variations in recruitment of
479 0.7, 1.0, and 2.0, respectively (Fig. 3).

480 Accuracy and precision decreased slightly when total temporal variation in recruitment
481 was allocated more to source × year-class variation than to year-class variation (Fig. 3). When
482 the allocation ratio between year-class class variation and source × year-class variation was 1:4
483 (i.e., 20% of total variation allocated to year-class variation and 80% of total variation allocated
484 to source × year-class variation), the median correlation and IQR in correlations were 0.837 and
485 0.122, respectively. Conversely with a 1:1 ratio the median correlation and IQR in correlations
486 were 0.850 and 0.111, respectively, and were 0.860 and 0.104 for a 4:1 ratio (Fig. 3).
487
488 **Sensitivity analyses**
489 Accuracy and precisions of the proposed estimation approach were insensitive to the
490 mortality scenarios that we considered as part of our sensitivity evaluations. Median correlations
491 and interquartile ranges in the correlations for these sensitivity scenarios deviated very little from
492 baseline simulation runs (Fig 3).
493 The estimation approach was insensitive to low aging error (i.e., the standard deviation of
494 estimated ages was modeled as a linear function of the expected true age with an intercept of 0
495 and a slope of 0.06) regardless of whether aging was assumed to be accurate or whether the
496 actual aging error matrix was incorporated in the estimation model (Fig. 4). For the scenario with
497 high aging error (i.e., the standard deviation of estimated ages was modeled as a linear function
498 of the expected true age with an intercept of 0 and a slope of 0.10), results depended on how
499 aging error was treated in the estimation model. When accurate aging was assumed in the
500 estimation model, median correlation in $\log_e$ recruitment declined by 0.03 to 0.05 and the
501 interquartile range in correlations increased by 0.01 to 0.02 across the range of evaluated factors
502 for the simulations (Fig. 4). When the actual aging error matrix was incorporated in the

503 estimation model, performance of the estimation approach with respect to both accuracy and
504 precision was worse compared to when aging was assumed to be accurate at small mixture
505 sample sizes (Fig. 4). At the smallest mixture sample sizes, median correlation in $\log_e$
506 recruitment declined by as much as 0.09 across the range of evaluated factor. With larger
507 mixture sample sizes, accuracy of the estimation approach when the actual aging error matrix
508 was incorporated in the approach was similar to when accurate aging was assumed (Fig. 4).
509 Precision of the estimation approach as measured by the interquartile range of the correlations
510 also improved with larger mixture sample sizes, although in all cases precision was worse than
511 when accurate aging was assumed (Fig. 4). In the follow-up simulations with mixture sample
512 sizes as large as 3,00 fish per hear, we found that incorporating the actual aging error matrix in
513 the estimation approach resulted in more accurate and precise estimates of $\log_e$ recruitment levels
514 compared to when accurate aging was incorrectly assumed in the estimation model (results not
515 shown).
516
517 **Empirical applications**
518 *Saginaw Bay, Lake Huron Walleye*.—All five MCMC chains were judged to have converged on
519 stationary and stable distributions for the relative recruitments for each source and year-class
520 combination. Examination of trace plots indicated that each of the MCMC chains were well
521 mixed for each relative recruitment estimate (Appendix C), and the Z-score test statistics ranged
522 from approximately -1.72 to 1.88. Effective sample sizes of the MCMC chains for all relative
523 recruitments were greater than 2,100. Overlaying the traceplots for all five MCMC chains
524 suggested that the chains had converged on the same stationary distributions for the relative
525 recruitments for each source and year-class combination (Appendix C). Additionally, the upper

95% confidence interval for the potential scale reduction factors calculated from the five MCMC chains for all relative recruitments was less than 1.1, suggesting that all chains had converged on the same stationary distributions. Effective sample sizes for the combined MCMC chains for all relative recruitments were greater than 10,900.

The pattern in relative recruitments that were generated from our estimation approach for Lake Huron closely corresponded with the recruitment estimates from the SCAA model by Fielder and Bence (2014) for the 2002 to 2006 year classes. The correlation between recruitment estimates was 0.921. Recruitment levels from both models increased from 2002 to 2003, but then decreased steadily from 2003 to 2006 (Fig. 5). There was also fairly strong correspondence in the estimated recruitments for Lakes Erie/St. Clair, although the correlation in recruitment levels for this source was 0.567 (Fig. 5). Our proposed approach predicted recruitment increased from 2002 to 2004 and then declined from 2004 to 2006. The SCAA model estimated a sharp increase in recruitment from 2002 to 2003 and an overall decline in recruitment from 2003 to 2006. Whereas our approached predicted that the recruitment level in 2004 was comparable to that of 2003, the SCAA model for Lakes Erie/St. Clair predicted that recruitment in 2004 was the second lowest of the time series (Fig. 5).

Northern Lake Michigan Lake trout.— All five MCMC chains converged on stationary and stable distributions for the relative recruitments for each source and year-class combination. Examination of trace plots indicated that each of the MCMC chains were well mixed for each relative recruitment estimate (Appendix C), and the Z-score test statistics ranged from approximately -1.23 to 1.88. Effective sample sizes of the MCMC chains for all relative recruitments were greater than 1,300. Overlaying the traceplots for all five MCMC chains

549 suggested that the chains had converged on the same stationary distributions for the relative
550 recruitments for each source and year-class combination (Appendix C). Additionally, the upper
551 95% confidence interval for the potential scale reduction factors calculated from the five MCMC
552 chains for all relative recruitments was less than 1.1, suggesting that all chains had converged on
553 the same stationary distributions. Effective sample sizes for the combined MCMC chains for all
554 relative recruitments were greater than 8,000.
555 Correspondence between recruitment estimates of the lake trout hatchery strains and the
556 actual stocking levels in Lake Michigan differed by strain. The strongest correspondence
557 between relative recruitments and stocking levels was for the Lewis Lake strain. The correlation
558 between estimated recruitments and stocking levels for the Lewis Lake strain was 0.444, with the
559 greatest discrepancy occurring for the 2007 year class (Fig 6). Our estimation approach predicted
560 increased recruitments from 2003 to 2005, but decreased recruitments from 2005 to 2008.
561 Conversely, the actual stocking rate of this hatchery strain for these year classes was fairly static
562 between 2003 and 2007 and then decreased in 2008. For the Lake Superior strain, the correlation
563 between estimated recruitment and stocking level was 0.334. Our estimation approach predicted
564 recruitment levels increased from 2003 to 2004 but then decreased from 2004 to 2008 (Fig. 6),
565 whereas the stocking rate for this hatchery strain increased from 2003 to 2006 and then
566 decreased from 2006 to 2008. For the Seneca Lake hatchery strain, there was a negative
567 correlation (-0.278) between our estimated recruitment levels and the stocking levels for this
568 strain, although this negative correlation was largely a result of a large difference between
569 relative recruitment and stocking level for the 2008 year class (Fig. 6). For the Green Lake
570 strain, there also was a negative correlation (-0.529) between relative recruitments and stocking

levels. Whereas the stocking levels of this hatchery strain decreased from 2003 to 2008, our estimation approach predicted slightly elevated recruitments in 2006 and 2007 (Fig. 6).

Discussion

Several quantitative approaches for indexing historical recruitment levels based exclusively on sampling of adult fish have been proposed and applied to fish populations (Guy and Willis 1995; Maceina 1997; Isermann et al. 2002; Tsehaye et al. 2016). The methodological approach proposed herein is similar to that of Tsehaye et al. (2016) in that it is meant for indexing recruitment for several sources simultaneously, which can provide beneficial information for management, as preserving genetic diversity is important for promoting resilience of populations to perturbations (Stephenson 1999). Both our approach and that of Tsehaye et al. (2016) are based on incorporating age or surrogates of age in commonly used model-based GSI methods. Thus, a prerequisite for both approaches is the availability of DNA markers that can be used to genotype individuals from both sources and mixtures. While this at one time may have been problematic, the development and widespread use of high throughput markers, such as single nucleotide polymorphisms (SNPs), have made it possible to easily identify large numbers of loci and cost-efficiently characterize variation in these loci for many individuals (Larson et al. 2014). Thus, our proposed approach, as well as that of Tsehaye et al. (2016), has the potential for broad applicability considering that the occurrence of intermixed fisheries is increasingly being recognized as a common feature in both marine and freshwater fish populations (Policansky and Magnuson 1998; Kerr et al. 2010; Brenden et al. 2015b).

Our proposed approach differs from that of Tsehaye et al. (2016) primarily in the assumed underlying dynamics of the source populations. The approach of Tsehaye et al. (2016)

was described as being applicable to long-lived species that spawn intermittently and that experience high mortality rates during early life stages, but that have low mortality rates after these critical early life periods. Such life histories were identified as likely to result in year-class strength changing fairly consistently on an annual basis. However, for many other species, recruitment levels can exhibit considerable inter-annual variation. For example, in Lake Erie walleye, 10-fold differences in estimated recruitment levels in adjacent years are common, and in some years differences in recruitment levels can be nearly 200-fold (WTG 2014). The approach we have proposed herein is intended for cases such as these, although there is nothing that would preclude its use in situations where recruitment levels changed consistently on an annual basis so long as sufficient data were available to index individual year classes. In describing their approach, Tsehaye et al. (2016) included situations where ages of individuals from mixtures were not available so lengths of individuals along with information on growth relationships for the sources were used as surrogates for age. The basis for this was that with long-lived and low mortality populations it might be difficult to obtain age estimates of from the mixture because it would require sacrificing individuals from the mixture, which might be problematic from a conservation perspective (Tsehaye et al. 2016). The estimation approach described herein could similarly be expanded to incorporate situations of using length as a surrogate if age estimates were difficult to obtain from fish collected from the mixture.

The simulations that were conducted as part of this research indicated that across a range of conditions, recruitment estimates from our estimation approach were strongly correlated with simulated recruitment levels. Both accuracy and precision of the recruitment estimates were influenced by mixture sample size and levels of genetic divergence among the sources. These same factors have been found to have the greatest influence on the performance of standard GSI

617 models (Brenden et al. 2015a). Our proposed estimation approach is an extension of standard
618 GSI models so this finding is perhaps not surprising. Accuracy and precision decreased when
619 more source populations were incorporated in analyses, which we attribute to there being simply
620 more opportunities for mistakes to arise when assigning individuals to sources. A longer
621 sampling duration also improved accuracy and precision of the estimation approach. We attribute
622 this finding to a longer sampling duration increasing the number of observations of the year
623 classes upon which to make inference. For example, with a six-year sampling duration, the
624 youngest year class in the first year of sampling will be able to be followed through to older ages
625 with each subsequent year of sampling, which results in more accurate estimates of initial
626 recruitment levels. We found that the approach was relatively unaffected by factors such as total
627 temporal variation, how temporal variation was allocated between year-class and source × year-
628 class interaction variation, and level of difference in source effects. The insensitivity to these
629 factors is encouraging as in actual applications it would be difficult to know what these factors
630 were prior to analyses, so it would be difficult to control for them. Conversely, mixture sample
631 size and sampling duration can be adjusted as needed, while genetic divergence between sources
632 can be assessed ahead of time.

633 The sensitivity analyses that we conducted as part of this research indicated that the
634 estimation approach was robust to assumptions about total mortality, but that large aging error
635 could influence recruitment estimates. The largest aging error we considered in our sensitivity
636 analyses was a case where only ~50% of older fish were accurately aged. Even for this scenario,
637 median recruitment correlations were in all cases greater than 0.60 suggesting that even with this
638 level of aging uncertainty there was still a fairly strong association between estimated and
639 assumed recruitment levels. We considered two approaches in our sensitivity analyses involving

aging error: one where aging was assumed to be accurate and one where the actual aging error matrix used to simulate observations from the mixture was incorporated in the estimation approach. Assuming that aging was accurate performed better at small mixture sample sizes, but at larger mixture sample sizes the two approaches performed similarly with respect to accuracy. At very high sample sizes, incorporating the actual aging error matrix that was used to simulate the mixture fishery data resulted in estimates that were very similar to simulations where no aging error occurred. Our explanation for why incorporating the actual aging error matrix used to simulate the mixture fishery data performed poorly at low mixture sample sizes samples is that with small samples the amount of aging error observed in the simulated mixture data could be considerably different from the actual aging error matrix because of the stochasticity in the generating process. Conversely, as mixture sample size increased, there was closer agreement between the observed aging error and the actual aging error matrix used to simulate the data. This result suggests there may be danger in simply assuming an aging error matrix and that if there is concern about error then age validation should be conducted for samples collected from the mixture. As well, with small sample sizes older age classes may be uncommon in the mixture and the incorporating of errors may make these observations highly influential data points. This, an additional option for dealing with high aging uncertainty would be to restrict analyses to younger fish that can presumably be aged with greater accuracy and perhaps sample over longer durations. Other quantitative approaches for indexing recruitment levels based on sampling of adult fish (e.g., Isermann et al. 2002) can also be affected by aging uncertainty, so the sensitivity of our proposed estimation approach to high levels of aging error should not be construed as a major hindrance to its adoption.

662 The empirical applications of our estimation approach found that there was close
663 agreement between our recruitment estimates and recruitment estimates from SCAA models for
664 walleye from Lake Huron and Lake Erie. However, the level of agreement between our estimates
665 and the stocking history for Lake Michigan for the lake trout example varied among the hatchery
666 strains. The discrepancy between our recruitment estimates and stocking level of the hatchery
667 strains is perhaps not surprising given stocking history and past research into ecological
668 differences among different hatchery strains. The stocking history of lake trout strains in the
669 Great Lakes is complex. Individual strains are stocked at different locations throughout the lake,
670 multiple strains are stocked at individual sites, and both fall fingerlings and spring yearlings are
671 stocked (FWS/GLFC 2010). Additionally, previous research on lake trout movement in the Great
672 Lakes has found dispersal rates from stocking sites to vary by area (Adlerstein et al. 2007),
673 between fall fingerlings and spring yearlings (Elrod 1987), and between strains (Elrod 1987;
674 Elrod et al. 1996a) and for habitat selection to differ between strains (Elrod et al. 1996b).
675 Additionally, mortality rates of hatchery strains may differ (McKee et al. 2004) possibly due to
676 differences in growth (Elrod et al. 1996b; McKee et al. 2004) and/or vulnerability and
677 susceptibility to attacks by sea lamprey *Petromyzon marinus* (Schneider et al. 1996). Large-scale
678 ecosystem changes in the Great Lakes, including major reductions in prey fish population
679 abundances in Lake Huron (Riley et al. 2008), also may be contributing to greater movement of
680 piscivores from Lake Huron to Lake Michigan (Clark et al. 2016). There is also the potential for
681 errors or omissions in the stocking database from the which the strain-specific stocking numbers
682 were compiled (FWS/GLFC 2010). Consequently, the total number of lake trout stocked of a
683 particular year class and hatchery strain in Lake Michigan in and of itself is likely not
684 representative of actual recruitment levels for the strains.

685 Our proposed estimation approach makes several assumptions and prior to its application
686 consideration should be given to their appropriateness. As with most model-based GSI
687 approaches, our approach assumes that the sources are in Hardy-Weinberg equilibrium. If the
688 source deviate from this assumption, then actual genotype frequency of individuals in the
689 mixture may deviate from expectation and this could influence recruitment estimates. Therefore,
690 sources should be tested for deviations from Hardy-Weinberg equilibrium prior to application of
691 our approach. An additional implicit assumption is that source-specific migration rates to the
692 mixture do not vary by age. As well, if individuals are collected from the mixture in more than
693 one sampling year, then the approach assumes that movement rates do not vary temporally. If
694 movements do vary by age or time, than recruitment estimates could be affected. If external
695 estimates of movement rates are available, than these rates could be incorporated in the
696 mathematical representation of the underlying population-specific processes affecting abundance
697 levels. Unless there is interest in making inter-population recruitment comparisons, knowing
698 how sources differ with respect to migration rates to the mixture is not necessary, although again
699 these rates could be incorporated in order for such comparisons to be conducted. Similarly, the
700 estimation approach assumes that vulnerability to the sampling gear used to collect individuals
701 from the mixture does not differ by age or over time although if external estimates of
702 vulnerability were available they could be incorporated in the model. As described here, the
703 approach assumes that all sources contributing to the mixture are included in the analysis. We
704 envision our proposed approach could be expanded to account for the possibility of unknown
705 sources contributing individuals to mixtures similar to how regular genetic stock identification
706 models have been expanded to account for this potential (Smouse et al. 1990; Prichard et al.
707 2000; Pella and Masuda 2006).

In conclusion, the estimation approach described and evaluated in this research is a general approach for evaluating relative recruitment levels of sources contributing to mixtures. It is based on the incorporation of ages in GSI models and can accommodate aging uncertainty, and could be expanded to use length as a surrogate for age or to accommodate the possibility of unknown sources. Although the specific applications we illustrate only evaluate within-source recruitment levels of populations that move to a common mixture, recruitment of sources relative to each other could also be addressed if additional information (e.g., rates of movement) were available. The approach is applicable to situations in which a full integrated stock assessment making use of genetic mixture data, is not feasible. We believe this will be common, given that often the time-series data needed for an integrated assessment is not available for all regions substantial numbers of fish migrate to for each source contributing to a particular mixture, and genetic data may also not be available for all such regions. The potential use of genetic data in full integrated stock assessments has been recognized (Spies and Punt 2015). While the probability equations we present for source genotype data and the joint age and genotype data for mixtures could be adapted for use in full integrated spatial stock assessments, we believe the capability for applications to estimating recruitment trends in the absence of the data needed for such assessments is a valuable contribution in its own right. The approach was found to provide accurate relative recruitment levels across a range of factor levels with mixture sample size and genetic divergence having the largest influence on performance results. Accuracy was reduced by high aging error aging. One strategy for reducing the consequences of aging error is to reduce the age range of individuals from the mixture that are incorporated in the analyses. We are of the opinion that this estimation approach could be applied in a variety of situations where sources are contributing individuals to mixtures and thus could be a widely applicable tool for managing

731 fish populations based on recreational, commercial, or assessment collections from mixed
732 fisheries.
733

734 Acknowledgements

735 This research was partially funded by Great Lakes Fishery Trust project 2009.1080.
736 Additional funding was provided by the Michigan Department of Natural Resources and other
737 contributing partners of the Michigan State University Quantitative Fisheries Center. The authors
738 thank W. Liu for his involvement in programming the simulation and estimation models. The
739 authors acknowledge A. Cook, K. Donner, M. Ebener, D. Fielder, J. Jonas, T. Kolb, S. Lennart,
740 K. Molton, C. Radek, C. Schelb, M. Thomas, and C. Vandergoot for their assistance in the
741 project. Computational work in support of this research was performed at Michigan State
742 University's High Performance Computing Center. This is publication 20YY-XX of the
743 Quantitative Fisheries Center. AD Model Builder code used for estimation and simulation can be
744 downloaded from figshare doi:XXXXXXXXXXX.
745

746 References

747 Adlerstein, S.A., Rutherford, E.S., Clevenger, J.A., Johnson, J.E., Clapp, D.F., and Woldt, A.P.
748 2007. Lake trout movements in U.S. waters of Lake Huron interpreted from coded wire
749 tag recoveries in recreational fisheries. J. Great Lakes Res. **33**(1):186-201.
750 doi:10.3394/0380-1330(2007)33[186:LTMIUW]2.0.CO;2.

751 Angers, B., L. Bernatchez, A. Angers, and L. Desgroseillers. 1995. Specific microsatellite loci
752 for brook charr reveal strong population subdivision on a microgeographic scale. J. Fish
753 Biol. **47**(Supplement A):177-185. doi:10.1111/j.1095-8649.1995.tb06054.x.
754 Berger, A.M., Jones, M.L., Zhao, Y., and Bence, J.R. 2012. Accounting for spatial population
755 structure at scales relevant to life history improves stock assessment: the case for Lake
756 Erie walleye *Sander vitreus.* Fish. Res. **115-116**(1):44-59.
757 doi:10.1016/j.fishres.2011.11.006.
758 Bjorndal, K.A., and Bolten, A.B. 2008. Annual variation in source contributions to a mixed
759 stock: implications for quantifying connectivity. Mol. Ecol. **17**(2):2185-2193. doi:
760 10.1111/j.1365-294X.2008.03752.x.
761 Borer, S.O., Miller, L.M., and Kapuscinski, A.R. 1999. Microsatellites in walleye *Stizostedion*
762 *vitreum.* Mol. Ecol. **8**(2):336-338. doi:10.1046/j.1365-294X.1999.00534.x.
763 Brenden, T.O., Bence, J.R., Lantry, B.F., Lantry, J.R., and Schaner, T. 2011. Population
764 dynamics of Lake Ontario lake trout during 1985-2007. N. Am. J. Fish. Manage.
765 **31**(5):962-979. doi:10.1080/02755947.2011.635241.
766 Brenden, T.O., Bence, J.R., and Szalai, E.B. 2012. An age-structured integrated assessment of
767 Chinook salmon population dynamics in Lake Huron's main basin since 1968. Trans.
768 Am. Fish. Soc. **141**(4):919-933. doi:10.1080/00028487.2012.675910.
769 Brenden, T.O., Bence, J.R., Liu, W., Tsehaye, I., and Scribner, K.T. 2015a. Comparison of the
770 accuracy and consistency of likelihood-based estimation routines for genetic stock
771 identification. Methods Ecol. Evol. **6**(7):817-827. doi:10.1111/2041-210X.12377.
772 Brenden, T.O., Scribner, K.T., Bence, J.R., Tsehaye, I., Kanefsky, J., Vandergoot, C.S., and
773 Fielder, D.G. 2015b. Contributions of Lake Erie and Lake St. Clair walleye populations

to the Saginaw Bay, Lake Huron recreational fishery: evidence from genetic stock identification. N. Am. J. Fish. Manage. **35**(3):567-577. doi:/10.1080/02755947.2015.1020079.

Clark, R.D., Jr., Bence, J.R., Claramunt, R.M., Johnson, J.E., Gonder, D., Legler, N.D., Robillard, S.R., and Dickinson, B.D. 2016. A spatially explicit assessment of changes in Chinook salmon fisheries in Lakes Michigan and Huron from 1986 to 2011. N. Am. J. Fish. Manage. **36**(5):1068-1083. doi:10.1080/02755947.2016.1185060.

Corander, J., Marttinen, P., and Mäntyniemi, S. 2006. A Bayesian method for identification of stock mixtures from molecular marker data. Fish. Bull. **104**(4):550-558. Available from http://fishbull.noaa.gov/1044/corander.pdf [accessed 9 December 2016].

Corell, H., Moksnes, P.O., Engqvist, A., Döös, K., and Jonsson, P.R. 2012. Depth distribution of larvae critically affects their dispersal and the efficiency of marine protected areas. Mar. Ecol. Prog. Ser. 467(1):29–46. doi:10.3354/meps09963.

Eldridge, W.H., Bacigalupi, M.D., Adelman, I.R., Miller, L.M., and Kapuscinski, A.R. 2002. Determination of relative survival of two stocked walleye populations and resident natural-origin fish by microsatellite DNA parentage assignment. Can. J. Fish. Aquat. Sci. **59**(2):282-290. doi:10.1139/f02-007.

Elrod, J.H. 1987. Dispersal of three strains of hatchery-reared lake trout in Lake Ontario. J. Great Lakes Res. **13**(2):157-167. doi:10.1016/S0380-1330(87)71639-6.

Elrod, J.H., O'Gorman, R., Schneider, C.P., and Schaner, T. 1996a. Geographical distributions of lake trout strains stocked in Lake Ontario. J. Great Lakes Res. **22**(4):871-883. doi:10.1016/S0380-1330(96)71008-0.

796 Elrod, J.H., O'Gorman, R., and Schneider, C.P. 1996b. Bathythermal distribution, maturity, and
797 growth of lake trout strains stocked in U.S. waters of Lake Ontario, 1978-1993. J. Great
798 Lakes Res. **22**(3):722-743. doi:10.1016/S0380-1330(96)70992-9.
799 Elrod, J.H., O'Gorman, R., and Schneider, C.P., Eckert, T.H., Schaner, T., Bowlby, J.N., and
800 Schleen, L. P. 1995. Lake trout rehabilitation in Lake Ontario. J. Great Lakes Res.
801 **21**(Supplement 1):83–107. doi:10.1016/S0380-1330(95)71085-1.
802 Fielder, D.G., and Bence, J.R. 2014. Integration of auxiliary information in statistical catch-at-
803 age (SCA) analysis of the Saginaw Bay stock of Walleye in Lake Huron. N. Am. J. Fish.
804 Manage. **34**(5):970-987. doi:10.1080/02755947.2014.938141.
805 Fogarty, M.J. 1993. Recruitment in randomly varying environments. ICES J. Mar. Sci.
806 **50**(3):247-260. doi:10.1006/jmsc.1993.1027.
807 Fournier, D.A., Skaug, H.J., Ancheta, J., Ianelli, J., Magnusson, A., Maunder, M., Nielsen, A.,
808 and Sibert, J. 2012. AD Model Builder: using automatic differentiation for statistical
809 inference of highly parameterized complex nonlinear models. Optim. Methods Softw.
810 **27**(2):233–249. doi:10.1080/10556788.2011.597854.
811 Frank, K.T., and Brickman, D. 2000. Allee effects and compensatory population dynamics
812 within a stock complex. Can. J. Fish. Aquat. Sci. **57**(3): 513-517. doi:10.1139/f00-024.
813 FWS/GLFC (U.S. Fish and Wildlife Service and Great Lakes Fishery Commission). 2010. Great
814 Lakes fish stocking database. USFWS, Region 3 Fisheries Program, and GLFC, Ann
815 Arbor, Michigan. Available from http://www.glfc.org/fishstocking/. [accessed 8 August
816 2017].
817 Gelman, A., and Rubin, D.B. 1992. Inference from iterative simulation using multiple sequences.
818 Stat. Sci. 7(4):457-511. doi10.1214/ss/1177011136.

819 Geweke, J. 1992. Evaluating the accuracy of sampling-based approaches to the calculation of
820 posterior moments. *Edited by* J. M. Bernado, J. O. Berger, A. P. Dawid, and A. F. M.
821 Smith. Bayesian Statistics 4. Oxford University Press, Oxford. pp. 169-193
822 doi:10.1.1.27.2952.
823 Guan, W., Cao, J., Chen, Y., and Cieri, M. 2013. Impacts of population and fishery spatial
824 structures on fishery stock assessment. Can. J. Fish. Aquat. Sci. **70**(8):1178-1189.
825 doi:10.1139/cjfas-2012-0364.
826 Guy, C.S., and Willis, D.W. 1995. Population and characteristics of black crappies in South
827 Dakota waters: a case for ecosystem-specific management. N. Am. J. Fish. Manage.
828 **15**(4):754-765. doi:10.1577/1548-8675(1995)015<0754:PCOBCI>2.3.CO;2.
829 Hansen, G.J.A., Carpenter, S.R., Gaeta, J.W., Hennessy, J.M., and Vander Zanden, M.J. 2015.
830 Predicting walleye recruitment as a tool for prioritizing management actions. Can. J.
831 Fish. Aquat. Sci. **72**(5):661-672. doi:10.1139/cjfas-2014-0513.
832 Hewitt, D.A., Lambert, D.M., Hoenig, J.M., Lipcius, R.N., Bunnell, D.B., and Miller, T.J. 2007.
833 Direct and indirect estimates of natural mortality for Chesapeake Bay blue crab. Trans.
834 Am. Fish. Soc. **136**(4):1030-1040. doi:10.1577/T06-078.1.
835 Hilborn, R., and Walters, C.J. 1992. Quantitative fisheries stock assessment: choice, dynamics,
836 and uncertainty. Chapman and Hall, New York. 570 pp.
837 Hutchings, J.A. 1996. Spatial and temporal variation in the density of northern cod and a review
838 of hypotheses for the stock's collapse. Can. J. Fish. Aquat. Sci. **53**(5):943-962.
839 doi:10.1139/f96-097.
840 Hutchings, J.A. 2000. Collapse and recovery of marine fishes. Nature **406**:882-885.
841 doi:10.1038/35022565.

842 Isermann, D.A., McKibbin, W.L., and Willis, D.W. 2002. An analysis of methods for
843 quantifying crappie recruitment variability. N. Am. J. Fish. Manage. **22**(4):1124-1135.
844 doi:10.1577/15488675(2002)022<1124:AAOMFQ>2.0.CO;2.
845 Kerr, L.A., Cadrin, S.X., and Secor, D.H. 2010. Simulation modelling as tool for examining the
846 consequences of spatial structure and connectivity on local and regional population
847 dynamics. ICES J. Mar. Sci. 67(2):1631-1639. doi: 10.1093/icesjms/fsq053.
848 King, T.L., Lubinski, B.A., Burnham-Curtis, M.K., Stott, W., and Morgan, R.P. 2012. Tools for
849 the management and conservation of genetic diversity in brook trout (*Salvelinus*
850 *fontinalis*): tri- and tetranucleotide microsatellite markers for the assessment of genetic
851 diversity, phylogeography, and historical demographics. Conserv. Genet. Resour.
852 **4**(3):539-543. doi:10.1007/s12686-012-9603-z.
853 Larson, W.A., Seeb, J.E., Pascal, C.E., Templin, W.D., and Seeb, L.W. 2014. Single-nucleotide
854 polymorphisms (SNPs) identified through genotyping-by-sequencing improve genetic
855 stock identification of Chinook salmon (*Oncorhynchus tshawytscha*) from western
856 Alaska. Can. J. Fish. Aquat. Sci. **71**(5):698-708. doi:10.1139/cjfas-2013-0502.
857 Li, Y., Bence, J.R., and Brenden, T.O. 2015. An evaluation of alternative assessment approaches
858 for intermixing fish populations: a case study with Great Lakes lake whitefish. ICES J.
859 Mar. Sci. **72**(1):70-81.doi:10.1093/icesjms/fsu057.
860 Ludsin, S.A., DeVanna, K.M., and Smith, R.E.H. 2014. Physical-biological coupling and the
861 challenge of understanding fish recruitment in freshwater lakes. Can. J. Fish. Aquat. Sci.
862 **71**(5):775-794. doi:10.1139/cjfas-2013-0512.

Mace, P.M. 1994. Relationships between common biological reference points used as thresholds and targets of fisheries management strategies. Can. J. Fish. Aquat. Sci. **51**(1):110-122.doi:10.1139/f94-013.

Maceina, M.J. 1997. Simple application of using residuals from catch-curve regressions to assess year-class strength in fish. Fish. Res. **32**(2):115-121. doi:10.1016/S0165-7836(97)00051-9.

McKee, P.C., Toneys, M.L., Hansen, M.J., and Holey, M.E. 2004. Performance of two strains of lake trout stocked in the midlake refuge of Lake Michigan. N. Am. J. Fish. Manage. **24**(4):1101–1111. doi:10.1577/M03-142.1.

Miller, T.J. 2007. Contribution of individual-based coupled physical-biological models to understanding recruitment in marine fish populations. Mar. Ecol. Prog. Ser. **347**(1):127-138. doi:doi:10.3354/meps06973.

Modeling Subcommittee, Technical Fisheries Committee. 2014. Technical Fisheries Committee Administrative Report 2014: Status of Lake Trout and Lake Whitefish Populations in the 1836 Treaty-Ceded Waters of Lake Superior, Huron and Michigan, with Recommended Yield and Effort Levels for 2014. Available from https://www.michigan.gov/documents/dnr/2014StatusStocksReport_465244_7.pdf [accessed 9 December 2016].

Myers, R., Mertz, A.G., and Bridson, J. 1997. Spatial scales of interannual recruitment variations of marine, anadromous, and freshwater fish. Can. J. Fish. Aquat. Sci. **54**(6):1400-1407. doi:10.1139/f97-045.

884 Myers, R.A., Rosenberg, A.A., Mace, P.M., Barrowman, N., and Restrep, V.R. 1994. In search
885 of thresholds for recruitment overfishing. ICES J. Mar. Sci. **51**(2):191-205.
886 doi:10.1006/jmsc.1994.1020.
887 Olsen, J.B., Bentzen, P., and Seeb, J.E. 1998. Characterization of seven microsatellite loci
888 derived from pink salmon. Mol. Ecol. 7(8):1087-1089. doi:10.1046/j.1365-
889 294X.1998.00401.x.
890 O'Reilly, P.T., Hamilton, L.C., McConnell, S.K., and Wright, J.W. 1996. Rapid analysis of
891 genetic variation in Atlantic salmon (*Salmo salar*) by PCR multiplexing of dinucleotide
892 and tetranucleotide microsatellites. Can. J. Fish. Aquat. Sci. **53**(10):2292-2298.
893 doi:10.1139/f96-192.
894 Pella, J.J., and Milner, G.B. 1987. Use of genetic marks in stock composition analysis. *Edited by*
895 N. Ryman and F. Utter, editors. Population genetics and fisheries management.
896 University of Washington Press, Seattle, Washington. pp. 247-276.
897 Pella, J., and Masuda, M. 2001. Bayesian methods for analysis of stock mixtures from genetic
898 characters. Fish. Bull. **99**(1):151–167. Available from http://fishbull.noaa.gov/991/13.pdf
899 [accessed 9 December 2016].
900 Pella, J., and Masuda, M. 2006. The Gibbs and splitmerge sampler for population mixture
901 analysis from genetic data with incomplete baselines. Can. J. Fish. Aquat. Sci. **63**(3):576-
902 596. doi:10.1139/f05-224.
903 Plummer, M., Best, N., Cowles, K., and Vines, K. 2006. CODA: convergence diagnosis and
904 output analysis for MCMC. R News 6(1):7-11. Available from https://cran.r-
905 project.org/doc/Rnews/Rnews_2006-1.pdf [accessed 9 December 2016].

906 Policansky, D., and Magnuson, J.J. 1998. Genetics, metapopulations, and ecosystem
907 management of fisheries. Ecol. Appl. **8**(Supplement 1):119-123. doi:10.1890/1051-
908 0761(1998)8[S119:GMAEMO]2.0.CO;2.
909 Pritchard, J.K., Stephens, M., and Donnelly, P. 2000. Inference of population structure using
910 multilocus genotype data. Genetics **155**(2):945-959.
911 Quinn, T.J., II, and Deriso, R.B. 1999. Quantitative fish dynamics. Oxford University Press, New
912 York. 542 pp.
913 R Core Team 2014. R: a language and environment for statistical computing. R Foundation for
914 Statistical Computing, Vienna, Austria.
915 Reiss, H., Hoarau, G., Dickey-Collas, M., and Wolff, W.J. 2009. Genetic population structure of
916 marine fish: mismatch between biological and fisheries management units. Fish Fish.
917 **10**(4):361-395. doi:10.1111/j.1467-2979.2008.00324.x.
918 Richards, L.J., Schnute, J.T., Kronlund, A.R., and Beamish, R.J. 1992. Statistical models for the
919 analysis of ageing error. Can. J. Fish. Aquat. Sci. **49**(9):1801-1815. doi:10.1139/f92-200.
920 Ricker, W.E. 1975. Computation and interpretation of biological statistics of fish populations.
921 Bull. Fish. Res. Board Can. No. 191 382 pp.
922 Riley, S.C., Roseman, E.F., Nichols, S.J., O'Brien, T.P., Kiley, C.S., and Schaeffer, J.S. 2008.
923 Deepwater demersal fish community collapse in Lake Huron. Trans. Am. Fish. Soc.
924 **137**(6):1879-1890. doi:10.1577/T07-141.1
925 Schneider, C.P., Owens, R.W., Bergstedt, R.A., and O'Gorman, R. 1996. Predation by sea
926 lamprey (*Petromyzon marinus*) on lake trout (*Salvelinus namaycush*) in southern Lake
927 Ontario, 1982-1992. Can. J. Fish. Aquat. Sci. **53**(9):1921-1932. doi:10.1139/f96-129.

928 Scribner, K.T., Gust, J.R., and Fields, R.L. 1996. Isolation and characterization of novel
929 microsatellite loci: cross-species amplification and population genetic applications. Can.
930 J. Fish. Aquat. Sci. **53**(4):833-841. doi:10.1139/f95-254.
931 Sissenwine, M.P. 1984. Why do fish populations vary? Pages 59-64 *in* R. M. May, editor.
932 Exploitation of marine communities. Springer-Verlag, Berlin. doi:10.1007/978-3-642-
933 70157-3_3.
934 Smouse, P.E., Waples, R.S., and Tworek, J.A. 1990. A genetic mixture analysis for use with
935 incomplete source population data. Can. J. Fish. Aquat. Sci. **47**(3):620-634. doi:
936 doi.org/10.1139/f90-070.
937 Stephenson, R.L. 1999. Stock complexity in fisheries management: a perspective of emerging
938 issue related to population sub-units. Fish. Res. **43**(1-3):247-249. doi:10.1016/S0165-
939 7836(99)00076-4.
940 Taylor, E.B., Redenbach, Z., Costello, A.B., Pollard, S.J., and Pacas, C.J. 2001. Nested analysis
941 of genetic diversity in northwestern North American char, Dolly Varden (*Salvelinus*
942 *malma*) and bull trout (*Salvelinus confluentus*). Can. J. Fish. Aquat. Sci. **58**(2):406-420.
943 doi:10.1139/f00-262.
944 Then, A.Y., Hoenig, J.M., Hall, N.G. and Hewitt, D.A. 2015. Evaluating the predictive
945 performance of empirical estimators of natural mortality using information on over 200
946 fish species. ICES J. Mar. Sci. **72**(1)82-92. doi: 10.1093/icesjms/fsu136.
947 Thorson, J.T., Jensen, O.P., and Zipkin, E.F. 2014. How variable is recruitment for exploited
948 marine fisheries? A hierarchical model for testing life history theory. Can. J. Fish. Aquat.
949 Sci. **71**(7):973-983. doi:10.1139/cjfas-2013-0645.

950 Tsehaye, I., Jones, M.L., Brenden, T.O., Bence, J.R., and Claramunt, R.M. 2014. Changes in the
951 salmonine community of Lake Michigan and their implications for predator-prey balance.
952 Trans. Am. Fish. Soc. **143**(2):420-437. doi:10.1080/00028487.2013.862176.
953 Tsehaye, I., Brenden, T.O., Bence, J.R., Liu, W., Scribner, K.T., Kanefsky, J., Bott, K., and
954 Elliott, R.F. 2016. Combining genetics with age/length data to estimate temporal changes
955 in year-class strength of sources contributing to mixtures. Fish. Res. **173**(3):236-249.
956 doi:10.1016/j.fishres.2015.09.004.
957 Van der Elst, W., Meyvisch, P., Alonso, A., Ensor, H.M., Weir, C.J., Molenberghs, G. 2017.
958 Surrogate: evaluation of surrogate endpoints in clinical trials. R package version 0.2.
959 Available from https://cran.r-project.org/package=Surrogate [accessed 7 August 201y].
960 Walleye Task Group (WTG). 2014. Report for 2013 by the Lake Erie Walleye task group. Great
961 Lakes Fishery Commission, Ann Arbor, Michigan. Available from
962 http://www.glfc.org/lakecom/lec/WTG_docs/annual_reports/WTG_report_2014.pdf
963 [accessed 9 December 2016].
964 Wirth, T., Saint-Laurent, R., and Bernatchez, L. 1999. Isolation and characterization of
965 microsatellite loci in the walleye (*Stizostedion vitreum*), and cross-species amplification
966 within the family Percidae. Mol. Ecol. **8**(11):1960-1962. doi:10.1046/j.1365-
967 294x.1999.00778-3.x.
968

969 Table 1. Assumed recruitment deviations (τ_i) values for sources for the simulations evaluating
970 the accuracy of our proposed estimation approach for indexing recruitment fluctuations in
971 populations contributing to mixtures. The τ_i values were constant across all simulations, whereas
972 the year-class ($\boldsymbol{\gamma}$) and source × year-class deviations ($\boldsymbol{\upsilon}$) were randomly generated for each
973 iteration.

6 Source Populations		12 Populations	
Low difference	High difference	Low difference	High difference
1) 0.833	1) 1.132	1) 0.783	1) 1.004
2) 0.634	2) 0.915	2) 0.698	2) 0.911
3) 0.387	3) 0.638	3) 0.604	3) 0.809
4) 0.056	4) 0.253	4) 0.501	4) 0.695
5) -0.440	5) -0.382	5) 0.387	5) 0.566
6) -1.470	6) -2.557	6) 0.257	6) 0.418
		7) 0.108	7) 0.245
		8) -0.067	8) 0.035
		9) -0.280	9) -0.231
		10) -0.550	10) -0.594
		11) -0.900	11) -1.171
		12) -1.519	12) -2.685

974

Fig. captions

Fig. 1. Map of Lakes Michigan, Huron, St. Clair, and Erie. The hashed area in Lake Michigan is the MM3 statistical district from which lake trout were collected for the empirical application of the proposed estimation approach for indexing recruitment fluctuations in populations contributing to mixtures. The hashed area in Lake Huron is Saginaw Bay from which walleye were collected. Arrows depict the contributions from source hatchery strains (lake trout) or spawning populations (walleye) to the mixtures. The placement of the lake trout strains on the map is not intended to convey locational information as to where strains originated from or where they were stocked.

Fig. 2. Flowchart of the framework used to simulate source genetic data, source relative recruitments and abundances, and observations from the source and mixtures for testing the proposed approach for estimating relative recruitments for source populations contributing to mixed fisheries. The dashed boxes and numbers correspond to steps in the simulation process described in the *Simulation factor levels* section.

Fig. 3. Boxplots of Pearson correlations between estimated and true $\log_e$ recruitment levels across the main-effect factor levels from the simulations conducted evaluating the performance of the proposed estimation approach. Boxplot whiskers extend to the most extreme correlation that is no more than 1.5 times the interquartile range of the correlations.

Fig. 4. Median and interquartile (IQR) range of correlations between estimated and true $\log_e$ recruitment levels from sensitivity analyses evaluating the robustness of the proposed estimation approach (Sensitivity scenarios: no aging uncertainty or total mortality variability = Base; random total mortality = Rand; autocorrelated total mortality = Auto;

998 population-specific total mortality = Pop; low aging error with accurate aging assumed =
999 AE06I, high aging error with accurate aging assumed = AE10I; low aging error
1000 incorporating aging error matrix = AE06C; high aging error incorporating aging error
1001 matrix = AE10C). The x-axis indicates the number of source populations, genetic
1002 divergence among the sources, and mixture fishery sample size.
1003 Fig. 5. Recruitment estimates and 95% highest posterior density intervals by year class for Lakes
1004 Huron and Lakes Erie/St. Clair walleye populations from the estimation approach
1005 proposed in this study based on collection of individuals from the Saginaw Bay
1006 recreational fishery (Fig. 1). Also plotted are the recruitment estimates for the same year
1007 classes from SCAA models constructed for the lakes (Fielder and Bence 2014; WTG
1008 2014).
1009 Fig. 6. Recruitment estimates 95% and highest posterior density intervals by year class for four
1010 hatchery strains of lake trout stocked into Lake Michigan from the estimation approach
1011 proposed in this study based on collection of individuals from the MM3 statistical district
1012 (Fig. 1). Also plotted are the numbers of lake trout stocked in northern Lake Michigan by
1013 hatchery strain for the same year classes.
1014

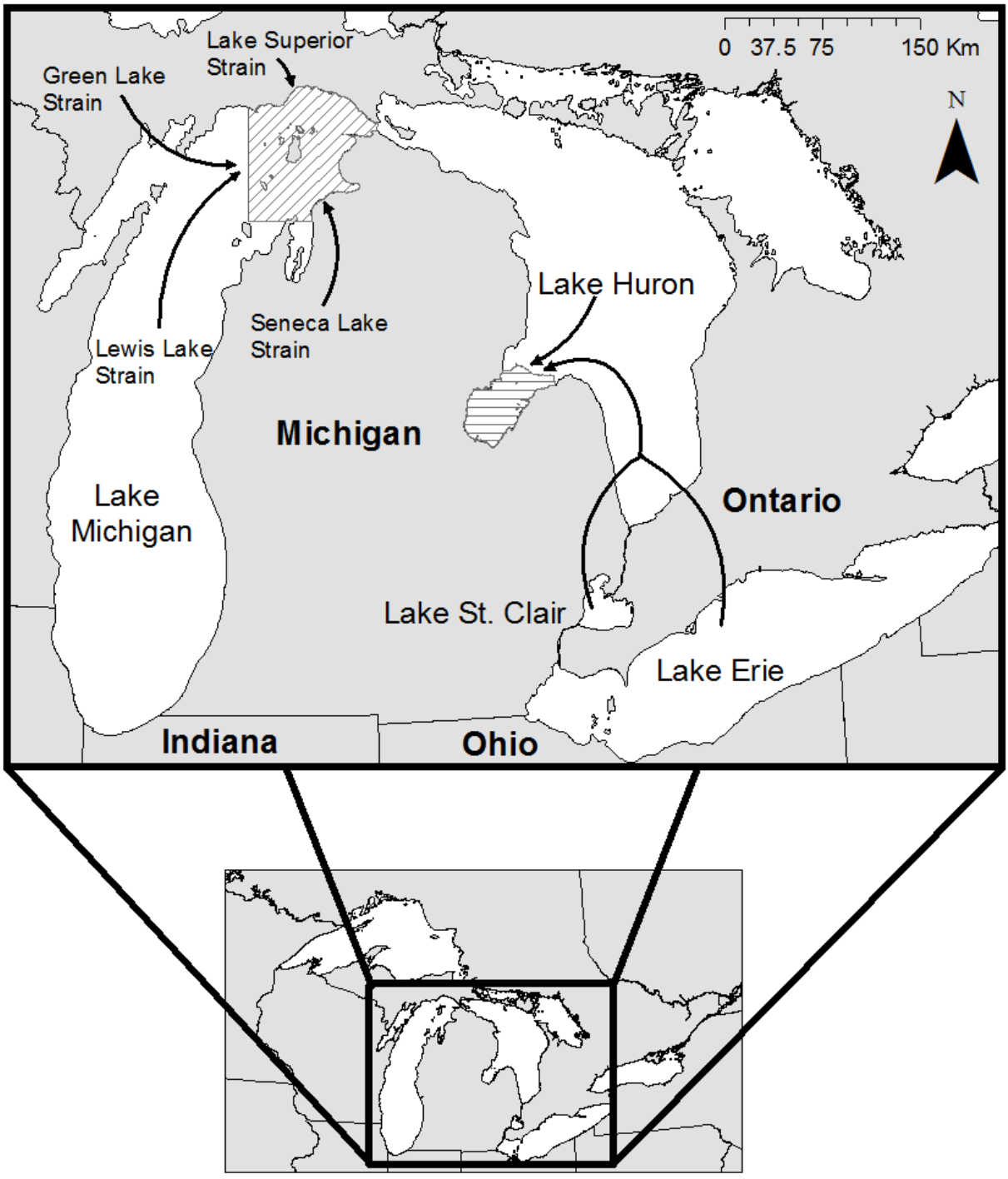
Lake Superior
Strain
Green Lake
Strain
0 37.5 75 150 Km
N
Lake Huron
Seneca Lake
Strain
Lewis Lake
Strain
Michigan
Lake
Michigan
Ontario
Lake St. Clair
Lake Erie
Indiana
Ohio

1015

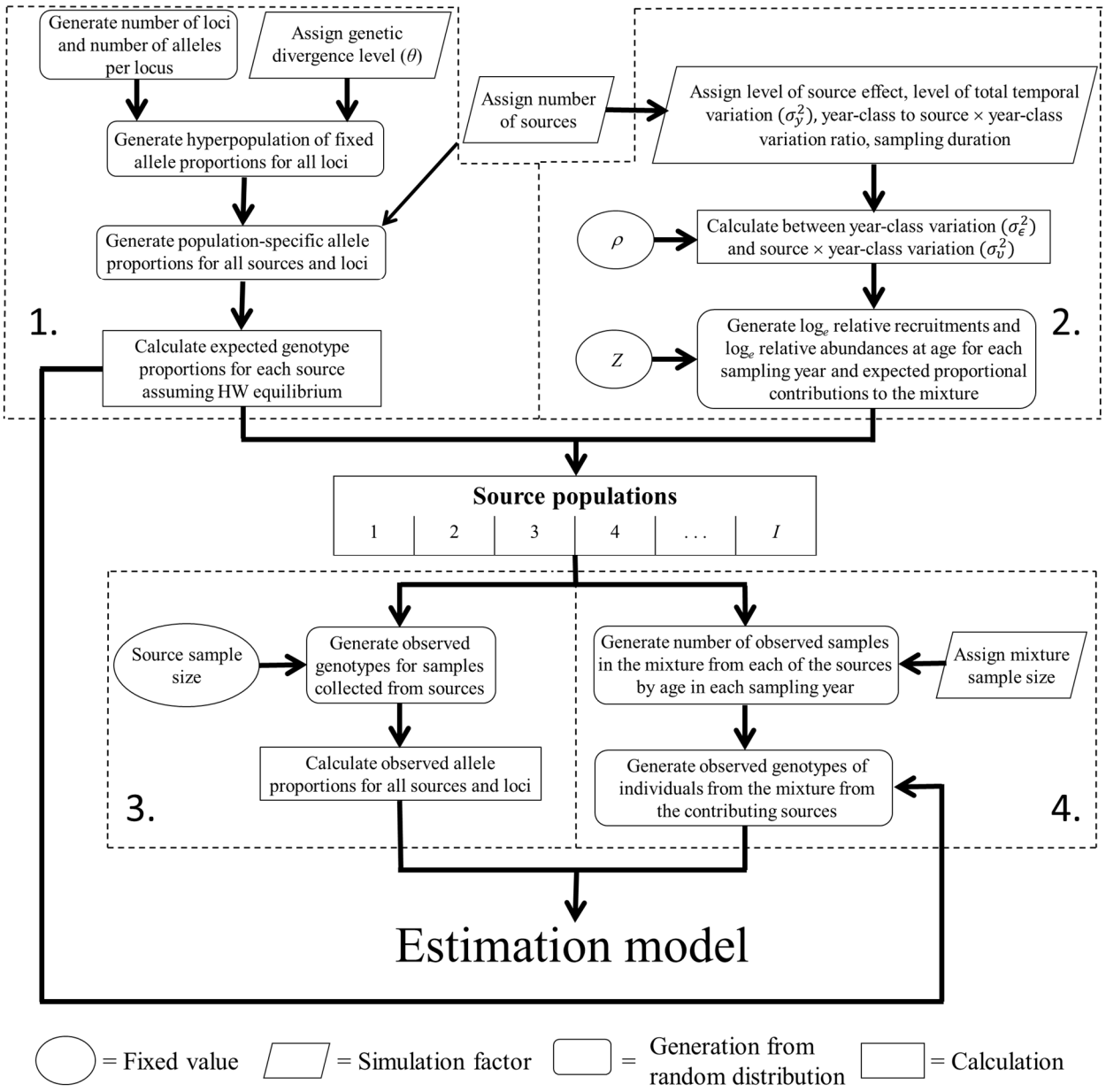
Generate number of loci and number of alleles per locus
Assign genetic divergence level (θ)
Generate hyperpopulation of fixed allele proportions for all loci
Assign number of sources
Assign level of source effect, level of total temporal variation (σ_y^2), year-class to source × year-class variation ratio, sampling duration
Generate population-specific allele proportions for all sources and loci
ρ
Calculate between year-class variation (σ_ϵ^2) and source × year-class variation (σ_v^2)
1.
Calculate expected genotype proportions for each source assuming HW equilibrium
Z
Generate $\log_e$ relative recruitments and $\log_e$ relative abundances at age for each sampling year and expected proportional contributions to the mixture
2.
Source populations
1
2
3
4
. . .
I
Source sample size
Generate observed genotypes for samples collected from sources
Generate number of observed samples in the mixture from each of the sources by age in each sampling year
Assign mixture sample size
Calculate observed allele proportions for all sources and loci
Generate observed genotypes of individuals from the mixture from the contributing sources
3.
4.
Estimation model
= Fixed value
= Simulation factor
= Generation from random distribution
= Calculation

1016

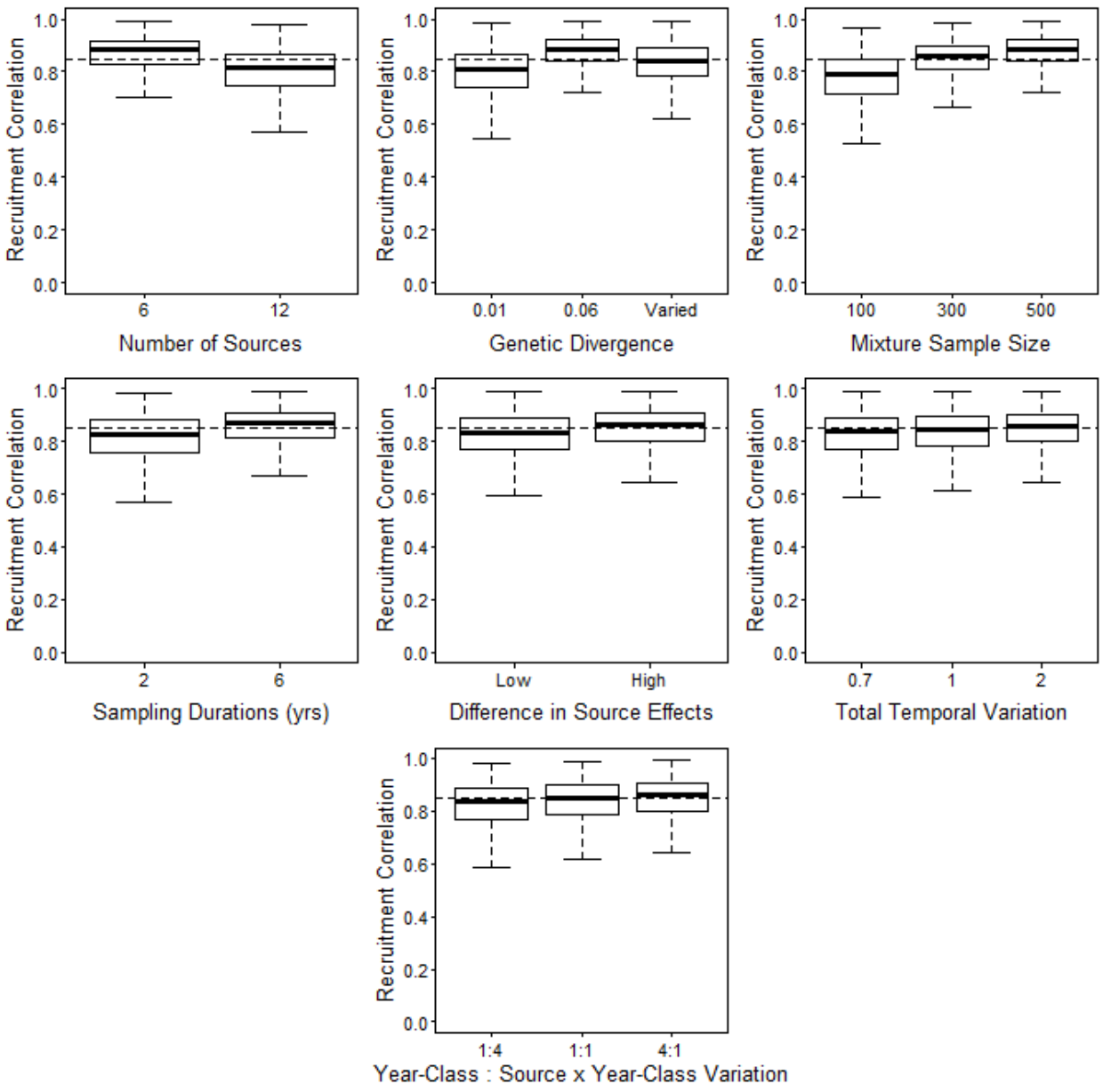
Recruitment Correlation
1.0
0.8
0.6
0.4
0.2
0.0
6
12
Number of Sources
0.01
0.06
Varied
Genetic Divergence
100
300
500
Mixture Sample Size
2
6
Sampling Durations (yrs)
Low
High
Difference in Source Effects
0.7
1
2
Total Temporal Variation
1:4
1:1
4:1
Year-Class : Source x Year-Class Variation

1017

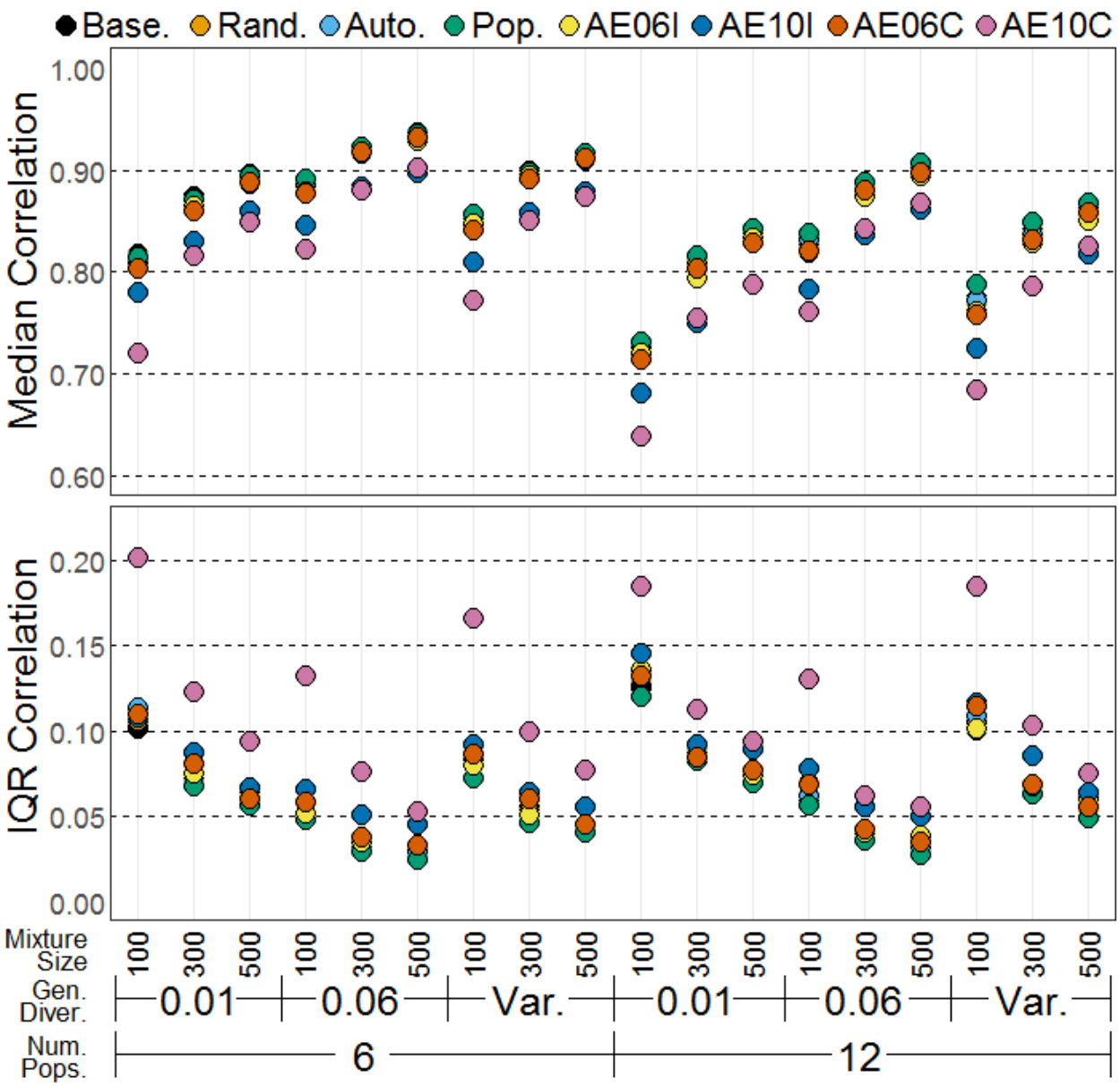
Base.
Rand.
Auto.
Pop.
AE06I
AE10I
AE06C
AE10C
Median Correlation
1.00
0.90
0.80
0.70
0.60
IQR Correlation
0.20
0.15
0.10
0.05
0.00
Mixture Size
100
300
500
Gen. Diver.
0.01
0.06
Var.
Num. Pops.
6
12

1018

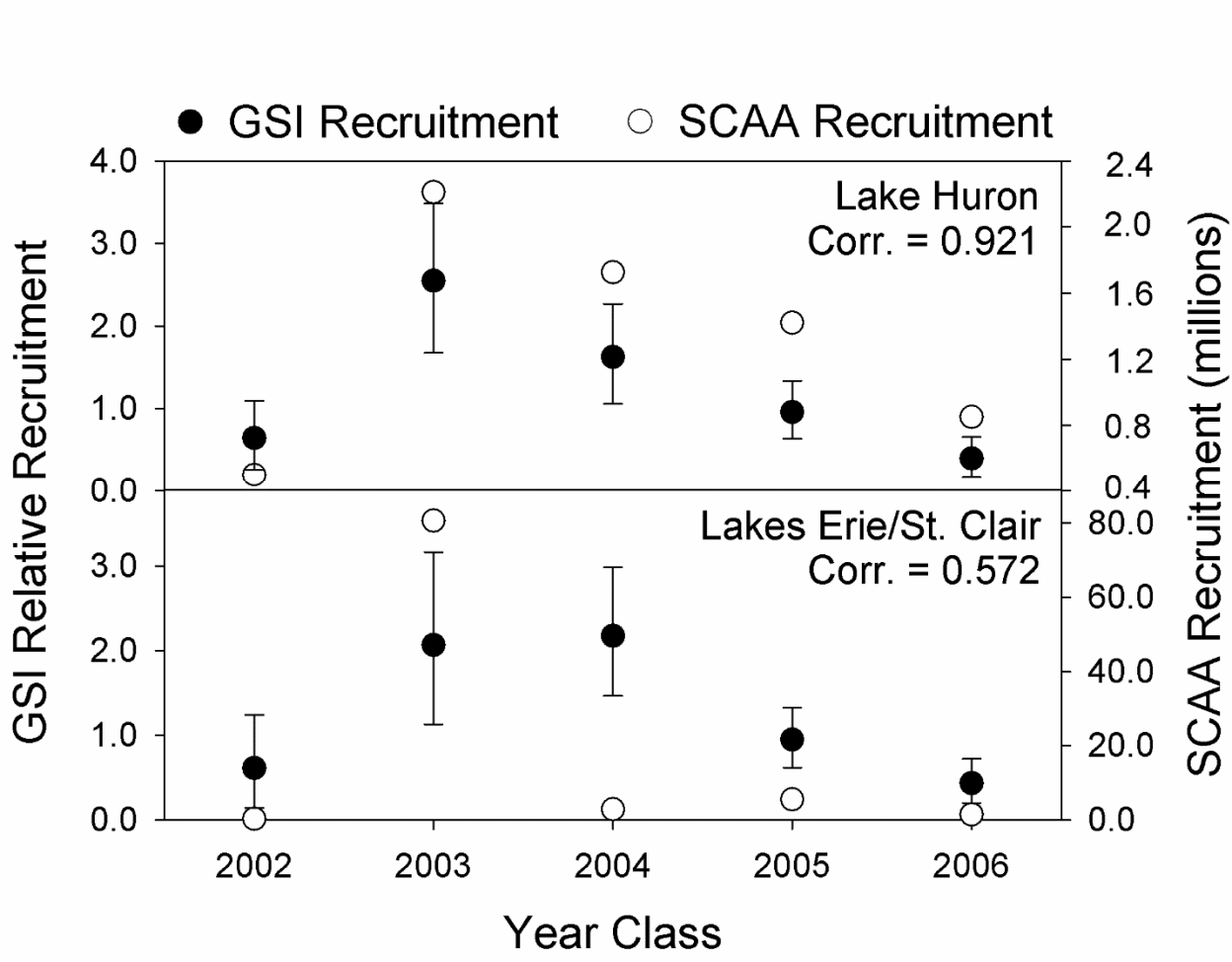
GSI Recruitment
SCAA Recruitment
Lake Huron
Corr. = 0.921
Lakes Erie/St. Clair
Corr. = 0.572
GSI Relative Recruitment
SCAA Recruitment (millions)
Year Class
2002
2003
2004
2005
2006
4.0
3.0
2.0
1.0
0.0
2.4
2.0
1.6
1.2
0.8
0.4
80.0
60.0
40.0
20.0
0.0

1019

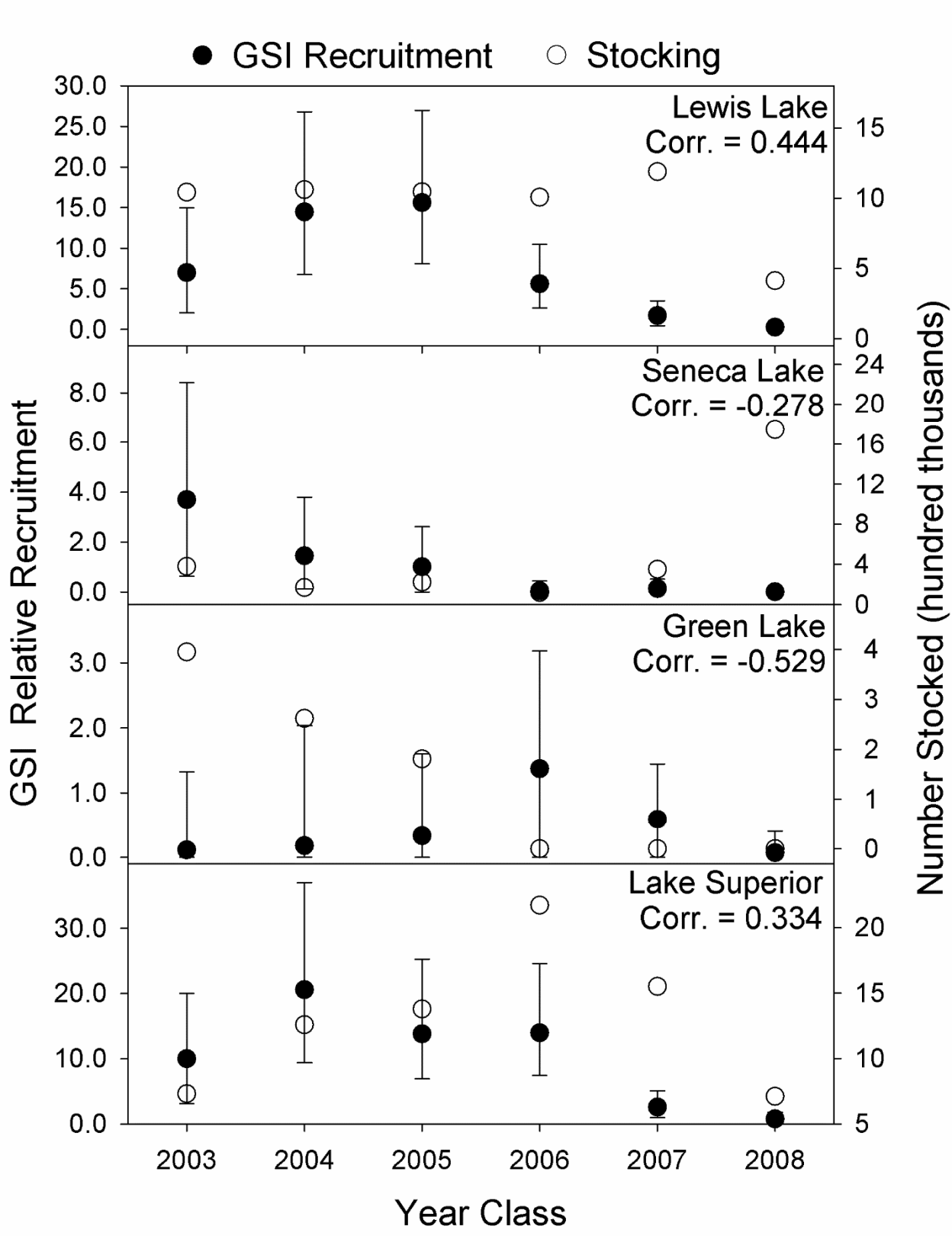
GSI Recruitment
Stocking
Lewis Lake
Corr. = 0.444
Seneca Lake
Corr. = -0.278
Green Lake
Corr. = -0.529
Lake Superior
Corr. = 0.334
GSI Relative Recruitment
Number Stocked (hundred thousands)
Year Class
2003
2004
2005
2006
2007
2008

1020

1021

Appendix A – Description of Source and Mixture Data Simulator

Source and mixture data were simulated following the hierarchical population structure and process of Guo et al. (2008). Allele frequencies for each source and locus were simulated from Dirichlet distributions using a two-stage approach (see Fig. A1 for an illustration of this approach). In the first stage, hyperpopulations of fixed allele frequencies for the h-th locus (ψ_h) were generated by a random draw from a Dirichlet distribution with concentration parameters set equal to 1 [i.e., $\psi_h \sim \mathrm{D}(\mathbf{1})$ (total number of concentration parameters equal the total number of alleles for the h-th locus)]. The simulated allele frequencies at the h-th locus for the i-th source were then generated by a random draw from a Dirichlet distribution with concentration parameters equal to $\left(\left(1-\theta\right)/\theta\right)\psi_h$. As noted by Guo et al. (2008), θ serves as a user-specified population divergence measure similar to Wright's F_{ST} (Wright 1965). When θ is small, the concentration parameters are large, which results in allele frequencies for the h-th locus that are very similar to the hyperpopulation of allele frequencies across all sources. Conversely when θ is large, the concentration parameters are small, which results in allele frequencies that can vary widely among the sources and from the hyperpopulation of allele frequencies.

For simulations where populations had varying divergence levels (see *Simulation factor levels*), actual allele frequencies were generated using a three-stage approach. In the first stage, we generated the ψ_h using the same method described above [i.e., $\psi_h \sim \mathrm{D}(\mathbf{1})$]. In the second stage, we generated two sub-hyperpopulations of allele frequencies based on random draws from Dirichlet distributions with concentration parameters equal to $\left(\left(1-\theta_{\mathrm{High}}\right)/\theta_{\mathrm{High}}\right)\psi_h$ (i.e., $\phi_{g,h} \sim D\left(\left(\left(1-\theta_{\mathrm{High}}\right)/\theta_{\mathrm{High}}\right)\psi_h\right)$) where $\phi_{g,h}$ denotes the allele frequencies for the h-th locus for the g-th sub-hyperpopulation and θ_{High} simply denotes a "high" genetic divergence factor so that

1044 expected genetic differences between the two sub-hyperpopulations would be high. We then
1045 generated the actual frequencies for the *h*-th locus for each source from random draws from
1046 Dirichlet distributions with concentration parameters equal to $\left(\left(1-\theta_{\text{Low}}\right)/\theta_{\text{Low}}\right)\phi_{g,h}$ where $\phi_{1,h}$ was
1047 used for one-half of the sources and $\phi_{2,h}$ was used for the other half (Tsehaye et al. 2016). Here,
1048 θ_{Low} simply denotes a "low" genetic divergence factor so that expected genetic differences of the
1049 source populations within a particular sub-hyperpopulations would be expected to be small. With
1050 this three-stage approach, each source would be expected to have relatively low levels of genetic
1051 divergence with half of the sources, and relatively high levels of genetic divergence with the
1052 other half of the sources.

1053 Observation error was incorporated in the generation of both allele relative frequencies
1054 from the sources as well the collection of individuals from the mixture. Genotypes of individuals
1055 collected from each of the sources were drawn randomly from multinomial distributions with
1056 probabilities equal to the expected genotype frequencies under Hardy-Weinberg equilibrium and
1057 the number of trials equal to the source sample size under evaluation (Fig. A1). These
1058 "observed" genotypes were then used to calculate allele relative frequencies for the sources. Data
1059 from the mixture were generated by two-stage multinomial random sampling. In the first stage,
1060 the number of sampled individuals from the mixture that came from each of the sources by age
1061 in each sampling year was determined by random draw from multinomial distribution with
1062 probabilities calculated based on the true relative abundances of each source and age for that
1063 examined scenario, and an assumed total mixture sample size. In the second stage, the genotypes
1064 of individuals from the mixture that came from each of the sources were generated by random
1065 draws from multinomial distributions with probabilities equal to the expected genotype

1066 frequencies for the sources and the number of trials equal to the number of individuals in the
1067 mixture that came from the sources.

1068 The true relative abundances at age by source for each simulation were obtained from
1069 equation 5, based on assumed $\boldsymbol{\tau}$, $\boldsymbol{\gamma}$, $\boldsymbol{\upsilon}$, and $Z_{i,a}$. In all base simulations $Z_{i,a}$ was fixed at 0.30, but in
1070 some sensitivity simulations stochasticity in $Z_{i,a}$ was incorporated in the operating model.
1071 Relative abundance at age for each source also depended on recruitment, through $\boldsymbol{\tau}$, $\boldsymbol{\gamma}$, and $\boldsymbol{\upsilon}$,
1072 based on equation 4. The source-specific deviations from grand mean recruitment (τ_i) were set at
1073 6 or 12 fixed levels that depended on the number of sources and the levels of difference in the
1074 source effects (see *Simulation factor levels*). Source-specific temporal variation in recruitment,
1075 as for the estimation model, consisted of the sum of year-class (i.e., coherent temporal)
1076 deviations (γ_y) and source × year-class (i.e., ephemeral temporal) deviations ($\upsilon_{i,y}$). The year-class
1077 deviations (γ_y) were simulated using a first-order autoregressive (AR1) process

1078
$$\begin{aligned} \gamma_y &= \rho\gamma_{y-1} + \varepsilon_y \\ \varepsilon_y &\sim N\left(0, \sigma_\varepsilon^2\right) \end{aligned}, \qquad \text{(A1)}$$

1079 where ρ is the auto-regressive coefficient. The source × year-class deviations ($\upsilon_{i,y}$) were
1080 simulated as a white-noise process:

1081
$$\upsilon_{i,y} \sim N\left(0, \sigma_\upsilon^2\right). \qquad \text{(A2)}$$

1082 The amount of total temporal recruitment variation (σ_y^2) and the ratio of how total
1083 temporal recruitment variation was allocated between year-class variation (σ_ε^2) and source ×
1084 year-class variation (σ_υ^2) were two of the factors that were explored during simulations to see
1085 how they affected accuracy and precision of the proposed estimation approach. Under an AR1
1086 process, the stationary variance for the year-class deviations is

$$\sigma_{\gamma}^2 = \frac{\sigma_{\varepsilon}^2}{1-\rho^2}. \quad \text{(A3)}$$

The overall temporal variation (σ_y^2) in simulated $\log_e$ recruitments was the sum of stationary variance for the year-class deviations and the source × year-class variation (σ_{υ}^2)

$$\sigma_y^2 = \sigma_{\gamma}^2 + \sigma_{\upsilon}^2. \quad \text{(A4)}$$

For all simulations, we assumed ρ was equal to 0.5. By assuming ρ and specifying the amount of total temporal recruitment variation and the ratio of how total temporal recruitment variation was allocated between year-class variation and source × year-class variation, we could use equations A3 and A4 to solve for σ_{ε}^2. This allowed us to simulate the time series of γ_y and $\upsilon_{i,y}$ according to equations A1 and A2 for a particular simulation scenario.

References

Guo, F., Dey, D.K., and Holsinger, K.E. 2008. A hierarchical Bayesian approach for estimating the origin of a mixed population. *Edited by* B. Clarke and J. K. Ghosal. Pushing the limits of contemporary statistics: contributions in honor of Jayanta K. Ghosh. Institute of Mathematical Statistics, Beachwood, Ohio. pp. 237-250 doi:10.1214/074921708000000174.

Tsehaye, I., Brenden, T.O., Bence, J.R., Liu, W., Scribner, K.T., Kanefsky, J., Bott, K., and Elliott, R.F. 2016. Combining genetics with age/length data to estimate temporal changes in year-class strength of sources contributing to mixtures. Fish. Res. **173**(3):236-249. doi:10.1016/j.fishres.2015.09.004.

Wright, S. 1965. The interpretation of population structure by F-statistics with special regard to systems of mating. Evolution **19**(3):395-420. doi:10.2307/2406450.

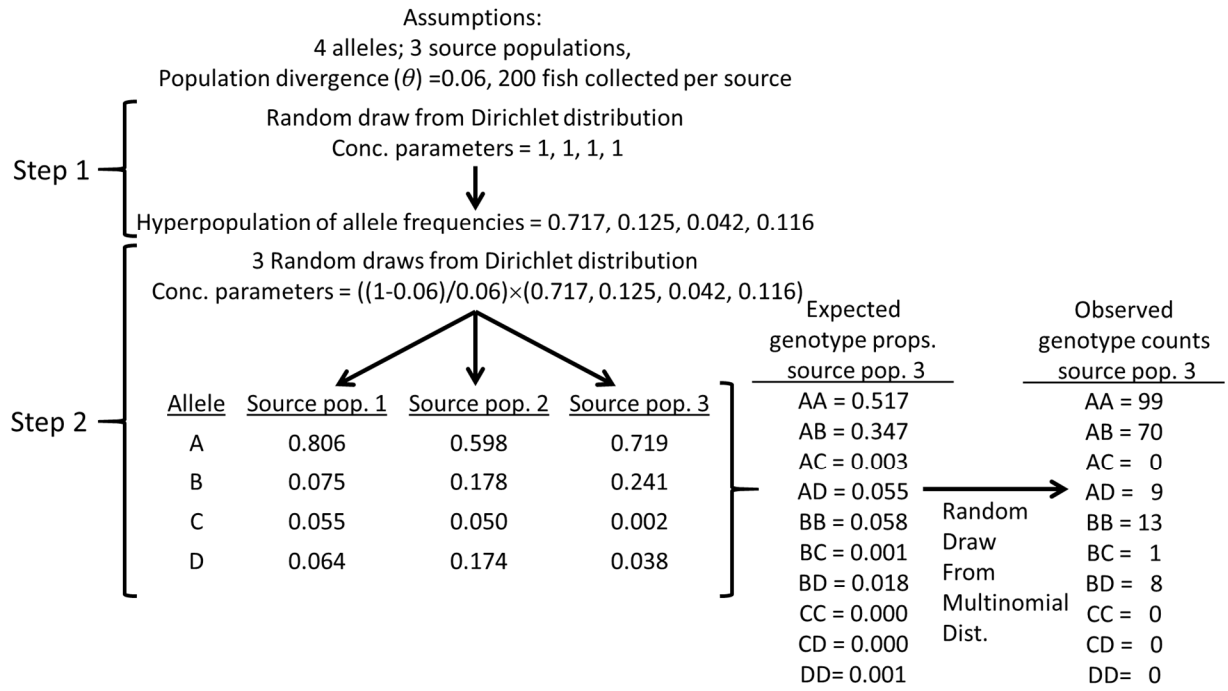

Fig. A1. Example illustration for how genetics data were generated for source populations. Illustration is for a single locus, assuming 4 alleles per locus, 3 source populations, a population divergence factor (j) = 0.06, and a source sample size of 200 fish. The depicted hyperpopulation allele proportions, the source-specific allele proportions, the expected genotype proportions for source 3, and the observed genotype counts for source 3 reflect just realizable random draws from the assumed distributions and are provided only for illustrative purposes.

Appendix B– Description of Lake Trout Hatchery Source Data and Genotyping

According to Page et al. (2003), lake trout stocking efforts in the Great Lakes have primarily been based on eight hatchery strains. For this research, we had tissue samples from six of these primary strains, as well as one additional hatchery strain. Hatchery strains from which we had tissue samples included four Lake Superior strains (Isle Royale, Apostle Island, Marquette, and Traverse Island), two Lake Michigan strains (Green Lake and Lewis Lake), and one Seneca Lake strain. Page et al. (2003) provides a discussion of the origin of these strains. These seven strains have comprised approximately 96% of the lake trout stocked in the northern Lake Michigan region from which mixture fishery tissue samples were obtained (USFWS and GLFC 2010). Fin tissue samples from these seven strains were collected by personnel affiliated with the hatcheries where broodstock were maintained. A total of 669 individuals from the seven hatchery strains were genotyped for the determination of allele frequencies.

Mixture and hatchery strain tissue samples were genotyped at 10 microsatellite loci: *Sfo*1, *Sfo*12, and *Sfo*18 (Angers et al. 1995); *Scou*19 (Taylor et al. 2001); *One*μ9 and *One*μ10 (Scribner et al. 1996); *Ogo*1a (Olsen et al. 1998); *Ssa*85 (O'Reilly et al. 1996); and *Sfo*-C24 and *Sfo*-D75 (King et al. 2012). PCR reactions were conducted in either 25 μl volumes using 100 ng of DNA (*Sfo*1, *Sfo*12, *Sfo*18, *Scou*19, *One*μ9, *One*μ10, *Ogo*1a, and *Ssa*85) or 10 μl volumes using 40 ng of DNA (*Sfo*-C24 and *Sfo*-D75). PCR buffer consisted of 10 mM Tris-HCl at pH 8.3, 50 mM KCl, 0.01% gelatin, 0.01% NP-40, and 0.01% Triton-X 100), and locus-specific volumes of dNTPs and $MgCl_2$ (Table B1). PCR cycling conditions also were locus-specific (Table B1). Fluorescently labeled forward primers and unlabeled reverse primers were used for *Sfo*1, *Sfo*12, *Sfo*18, *Scou*19, *One*μ9, *One*μ10, *Ogo*1a, and *Ssa*85, whereas infrared fluorescently labeled

forward primers and unlabeled reverse primers were used for *Sfo*-C24 and *Sfo*-D75. For *Sfo*1, *Sfo*12, *Sfo*18, *Scou*19, *One*μ9, *One*μ10, *Ogo*1a, and *Ssa*85, PCR products were separated by size on a denaturing 6.0% polyacrylamide gel and visualized using a Hitachi FMBIO II Multi-Vew scanner (Hitachi Solutions America, San Bruna, CA). For *Sfo*-C24 and *Sfo*-D75, PCR products were separated by size on a denaturing 6.5% polyacrylamide gel and visualized using a LI-COR 4300 DNA Analyzer (LI-COR Biosciences, Lincoln, NE).

Number of alleles, allelic richness, observed heterozygosity (H_o), and expected heterozygosity (H_e) for each locus and hatchery strain are shown in Table B2. Each hatchery strain at each locus was found to be in HW equilibrium at an error rate of 0.000714 after Bonferroni correction (Table B2). Of the 315 possible pairwise combinations between loci for the hatchery strains, of hatchery strains and loci, only two pairings were found to be in linkage disequilibrium (non-random association between alleles) at an error rate of 0.000159 after Bonferroni correction. These combinations were the following: Isle Royale strain: *Ssa*85 and *Sfo-D*75; Green Lake strain: *Sfo*18 and *Sfo-C*24. Because linkage disequilibriums for particular locus combinations were only found in a single hatchery strain, we did not feel it was necessary to exclude any of the loci for which linkage disequilibrium was detected.

Pairwise F_{ST} values between hatchery strains ranged from 0.001 for the Marquette and Apostle Island hatchery strains to 0.090 for the Seneca Lake and Lewis Lake strains (Table B3). The 4 hatchery strains from Lake Superior had the lowest pairwise F_{ST} values among all the assessed combinations. F_{ST} values did not exceed 0.0180 for any of the Lake Superior hatchery strain pairs (Table B3). Each of the pairwise F_{ST} values was significantly different from 0 at $P<0.0001$; however, conducting 100% mixture simulations in ONCOR (Kalinowski et al. 2007), which implements the simulation approach of Anderson et al. (2008) and involves repeated

(number of iterations = 1,000) generation of mixtures comprised solely of fish from just one of the hatchery strains, indicated there was some difficulty in differentiating between the Lake Superior strains based on the data available. Accuracies from the 100% mixture simulations for the Lake Superior strains ranged from around 72 to 85%. In other applications, 90% accuracy thresholds from 100% mixture simulations have been the target for sources prior to genetic stock identification analyses to reduce the possibility of biases in contribution estimates (Seeb and Crane 1999; Beacham et al. 2012; Brenden et al 2015). Because misallocation between Lake Superior hatchery strains could affect the accuracy of the recruitment estimates from our estimation approach, we chose to combine all Lake Superior hatchery strains together for the purpose of estimating recruitment levels. Thus, our analyses involved a total of four hatchery strains: Lake Superior, Green Lake, Lewis Lake, and Seneca Lake. Accuracy from 100% mixture simulations for these four strains ranged from approximately 95 to 100%.

LITERATURE CITED

Anderson, E.C., Waples, R.S., and Kalinowski, S.T. 2008. An improved method for predicting the accuracy of genetic stock identification. Can. J. Fish. Aquat. Sci. 65(7):1475-1486. doi:10.1139/F08-049.

Angers, B., L. Bernatchez, A. Angers, and L. Desgroseillers. 1995. Specific microsatellite loci for brook charr reveal strong population subdivision on a microgeographic scale. J. Fish Biol. **47**(Supplement A):177-185. doi:10.1111/j.1095-8649.1995.tb06054.x.

Beacham, T.D., Wallace, C.G., Le, K.D., and Beere, M. 2012. Population structure and run timing of steelhead in the Skeena River, British Columbia. N. Am. J. Fish. Manage. **32**(2):262-275. doi:10.1080/02755947.2012.675953.

1187 Brenden, T.O., Scribner, K.T., Bence, J.R., Tsehaye, I., Kanefsky, J., Vandergoot, C.S., and
1188 Fielder, D.G. 2015. Contributions of Lake Erie and Lake St. Clair walleye populations to
1189 the Saginaw Bay, Lake Huron recreational fishery: evidence from genetic stock
1190 identification. N. Am. J. Fish. Manage. **35**(3):567-577.
1191 doi:/10.1080/02755947.2015.1020079.
1192 Kalinowski, S.T., Manlove, K.R., and Taper, M.L. 2007. ONCOR: a computer program for
1193 genetic stock identification. Montana State University, Bozeman. Available at
1194 http://www.montana.edu/kalinowski/Software/ONCOR.htm [accessed 9 December
1195 2016].
1196 King, T.L., Lubinski, B.A., Burnham-Curtis, M.K., Stott, W., and Morgan, R.P. 2012. Tools for
1197 the management and conservation of genetic diversity in brook trout (*Salvelinus*
1198 *fontinalis*): tri- and tetranucleotide microsatellite markers for the assessment of genetic
1199 diversity, phylogeography, and historical demographics. Conserv. Genet. Resour.
1200 **4**(3):539-543. doi:10.1007/s12686-012-9603-z.
1201 Olsen, J.B., Bentzen, P., and Seeb, J.E. 1998. Characterization of seven microsatellite loci
1202 derived from pink salmon. Mol. Ecol. 7(8):1087-1089. doi:10.1046/j.1365-
1203 294X.1998.00401.x.
1204 O'Reilly, P.T., Hamilton, L.C., McConnell, S.K., and Wright, J.W. 1996. Rapid analysis of
1205 genetic variation in Atlantic salmon (*Salmo salar*) by PCR multiplexing of dinucleotide
1206 and tetranucleotide microsatellites. Can. J. Fish. Aquat. Sci. **53**(10):2292-2298.
1207 doi:10.1139/f96-192.

1208 Page, K.S., Scribner, K.T., Bennett, K.R., Garzel, L.M., and Burnham-Curtis, M.K. 2003.
1209 Genetic assessment of strain-specific sources of lake trout recruitment in the Great Lakes.
1210 Trans. Am. Fish. Soc. **132**(5):877-894. doi: 10.1577/T02-092.
1211 Scribner, K.T., Gust, J.R., and Fields, R.L. 1996. Isolation and characterization of novel
1212 microsatellite loci: cross-species amplification and population genetic applications. Can.
1213 J. Fish. Aquat. Sci. **53**(4):833-841. doi:10.1139/f95-254.
1214 Seeb, L. W., and Crane, P.A. 1999. Allozymes and mitochondrial DNA discriminate Asian and
1215 North American populations of chum salmon in mixed stock fisheries along the south
1216 coast of the Alaska peninsula. Trans. Am. Fish. Soc. **128**(1):88-103. doi:10.1577/1548-
1217 8659(1999)128<0088:AAMDDA>2.0.CO;2.
1218 Taylor, E.B., Redenbach, Z., Costello, A.B., Pollard, S.J., and Pacas, C.J. 2001. Nested analysis
1219 of genetic diversity in northwestern North American char, Dolly Varden (*Salvelinus*
1220 *malma*) and bull trout (*Salvelinus confluentus*). Can. J. Fish. Aquat. Sci. **58**(2):406-420.
1221 doi:10.1139/f00-262.
1222 Weir, B.S., and Cockerham, C.C. 1984. Estimating *F*-statistics for the analysis of population
1223 structure. Evolution **38**(6):1358–1370. doi:10.2307/2408641.
1224
1225

Table B1. Amplification conditions for the 10 microsatellites used to genotype lake trout hatchery strains and individuals collected from the northern Lake Michigan mixture fishery. The volumes of dNTP and MgCl2 represent amounts added to PCR buffer.

Locus	dNTP volume (mM)	MgCl2 volume (mM)	Cycling Condition
*Sfo*1	0.08	2.5	94°C for 2 m (1 cycle) - denaturing 94°C for 1 m (35 cycles) - denaturing 60°C for 1 m - annealing 72°C for 1 m - extension
*Sfo*12	0.2	3.0	94°C for 2 m (1 cycle) - denaturing 94°C for 1 m (35 cycles) - denaturing 57°C for 1 m - annealing 72°C for 1 m - extension
*Sfo*18	0.2	3.0	94°C for 2 m (1 cycle) - denaturing 94°C for 1 m (40 cycles) - denaturing 50°C for 1 m - annealing 72°C for 1 m - extension
*Scou*19	0.2	2.5	94°C for 2 m (1 cycle) - denaturing 94°C for 1 m (35 cycles) - denaturing 46°C for 1 m - annealing 72°C for 1 m - extension
*One*µ9	0.2	2.5	94°C for 2 m (1 cycle) - denaturing 94°C for 1 m (35 cycles) - denaturing 54°C for 1 m - annealing 72°C for 1 m - extension
*One*µ10	0.2	2.5	94°C for 2 m (1 cycle) - denaturing 94°C for 1 m (35 cycles) - denaturing 45°C for 1 m - annealing 72°C for 1 m - extension
*Ogo*1a	0.2	1.5	94°C for 2 m (1 cycle) - denaturing 94°C for 1 m (35 cycles) - denaturing 52°C for 1 m - annealing 72°C for 1 m - extension
*Ssa*85	0.2	2.5	94°C for 2 m (1 cycle) - denaturing 94°C for 1 m (35 cycles) - denaturing 56°C for 1 m - annealing 72°C for 1 m - extension
Sfo-C24	0.2	2.75	94°C for 2 m (1 cycle) - denaturing 94°C for 1 m (33 cycles) - denaturing 54°C for 1 m - annealing 72°C for 1 m - extension

Sfo-D75	0.2	4.00	94°C for 2 m (1 cycle) - denaturing 94°C for 1 m (32 cycles) - denaturing 54°C for 1 m - annealing 72°C for 1 m and 15 s - extension 72°C for 5 m (1 cycle) - extension

1229

1230

Table B2. Genetic variation in lake trout hatchery strains at 10 microsatellite loci screened for this study. Total number of alleles, allelic richness, expected (H_e) and observed (H_o) heterozygosities, and *P*-values for Hardy-Weinberg equilibrium tests at individual loci for each hatchery strains and combined across hatchery strains (total number of alleles and allelic richness only) are listed. Also shown are the results when all Lake Superior hatchery strains are combined. Three genetic fixation indices (Weir and Cockerham 1984) for each loci and for all loci are also displayed (F_{ST}=mean genetic divergence between pairs of spawning populations, F_{IS}=mean genetic differentiation within spawning populations; F_{IT}=deviation in the total sample). For the genetic fixation indices calculated for all loci, 95% confidence limits for the indices were derived by bootstrapping. NC=Not calculated

Locus	Hatchery Strain	Alleles	Allelic Richness	H_e	H_o	HWE *P*-value	F_{ST}	F_{IS}	F_{IT}
Sfo1	All strains	3	2.9	NC	NC	NC	0.080	0.010	0.089
	Isle Royale	3	3.0	0.16	0.17	1.000			
	Apostle Island	3	3.0	0.20	0.21	1.000			
	Marquette	3	3.0	0.15	0.16	1.000			
	Traverse Island	3	3.0	0.31	0.28	0.028			
	Green Lake	3	2.7	0.09	0.09	1.000			

	Lewis Lake	2	2.0	0.05	0.03	0.053			
	Seneca Lake	3	2.7	0.42	0.41	0.430			
	All Lake Superior strains	3	3.0	0.20	0.20	0.312			
Sfo12	All strains	5	4.1	NC	NC	NC	0.025	-0.003	0.023
	Isle Royale	4	3.7	0.31	0.28	0.449			
	Apostle Island	4	4.0	0.26	0.29	0.912			
	Marquette	5	4.9	0.24	0.24	0.575			
	Traverse Island	4	4.0	0.39	0.35	0.113			
	Green Lake	3	3.0	0.27	0.31	0.702			
	Lewis Lake	4	3.9	0.15	0.15	1.000			
	Seneca Lake	3	3.0	0.38	0.37	0.330			
	All Lake Superior strains	5	4.4	0.30	0.29	0.285			
Sfo18	All strains	11	7.6	NC	NC	NC	0.068	-0.089	-0.016
	Isle Royale	9	8.3	0.63	0.66	0.074			

	Apostle Island	7	6.3	0.61	0.66	0.612			
	Marquette	7	6.2	0.57	0.61	0.749			
	Traverse Island	6	6.0	0.56	0.58	0.850			
	Green Lake	6	5.6	0.58	0.70	0.013			
	Lewis Lake	7	6.3	0.63	0.70	0.953			
	Seneca Lake	4	4.0	0.41	0.45	0.754			
	All Lake Superior strains	10	7.7	0.60	0.63	0.405			
Scou19	All strains	12	8.3	NC	NC	NC	0.023	-0.001	0.023
	Isle Royale	9	8.4	0.65	0.64	0.544			
	Apostle Island	7	6.9	0.69	0.62	0.555			
	Marquette	10	8.8	0.71	0.73	0.005			
	Traverse Island	7	7.0	0.73	0.71	0.520			
	Green Lake	8	7.3	0.76	0.81	0.445			
	Lewis Lake	7	7.0	0.69	0.70	0.465			
	Seneca Lake	7	6.3	0.72	0.74	0.760			

	All Lake Superior strains	11	8.2	0.70	0.67	0.375			
One9	All strains	6	3.8	NC	NC	NC	0.008	0.007	0.015
	Isle Royale	3	3.0	0.13	0.12	0.353			
	Apostle Island	3	3.0	0.13	0.13	1.000			
	Marquette	6	5.7	0.20	0.21	1.000			
	Traverse Island	3	3.0	0.08	0.09	1.000			
	Green Lake	2	2.0	0.15	0.14	0.486			
	Lewis Lake	3	3.0	0.10	0.09	0.219			
	Seneca Lake	3	2.7	0.15	0.15	0.082			
	All Lake Superior strains	6	4.3	0.14	0.14	0.881			
One10	All strains	4	2.2	NC	NC	NC	0.038	-0.055	-0.05
	Isle Royale	2	2.0	0.26	0.24	0.454			
	Apostle Island	2	2.0	0.31	0.36	0.181			
	Marquette	2	2.0	0.23	0.26	0.349			

	Traverse Island	3	3.0	0.29	0.23	0.228			
	Green Lake	2	2.0	0.30	0.31	1.000			
	Lewis Lake	3	2.7	0.48	0.53	0.181			
	Seneca Lake	2	2.0	0.38	0.41	0.417			
	All Lake Superior strains	3	2.2	0.27	0.27	0.867			
Ogo1a	All strains	8	4.3	NC	NC	NC	0.098	-0.002	0.096
	Isle Royale	3	3.0	0.33	0.36	0.545			
	Apostle Island	4	3.7	0.48	0.41	0.166			
	Marquette	3	3.0	0.44	0.44	0.212			
	Traverse Island	4	4.0	0.38	0.35	0.024			
	Green Lake	4	3.7	0.53	0.60	0.437			
	Lewis Lake	6	5.7	0.65	0.63	0.188			
	Seneca Lake	4	3.7	0.60	0.62	0.678			
	All Lake Superior strains	4	3.5	0.42	0.39	0.073			

Ssa85	All strains	7	4.3	NC	NC	NC	0.057	-0.068	-0.007
	Isle Royale	4	4.0	0.64	0.64	0.030			
	Apostle Island	5	4.7	0.54	0.63	0.203			
	Marquette	4	4.0	0.47	0.48	0.642			
	Traverse Island	4	4.0	0.49	0.49	0.652			
	Green Lake	4	3.9	0.54	0.57	0.717			
	Lewis Lake	4	3.7	0.62	0.67	0.603			
	Seneca Lake	3	2.7	0.50	0.58	0.120			
	All Lake Superior strains	5	4.2	0.55	0.57	0.118			
Sfo-C24	All strains	4	3.1	NC	NC	NC	0.042	-0.038	0.005
	Isle Royale	3	3.0	0.55	0.48	0.117			
	Apostle Island	3	3.0	0.59	0.57	0.255			
	Marquette	3	3.0	0.51	0.64	0.001			
	Traverse Island	3	3.0	0.61	0.58	0.928			
	Green Lake	3	3.0	0.32	0.33	1.000			

	Lewis Lake	3	3.0	0.47	0.58	0.063			
	Seneca Lake	4	3.7	0.52	0.55	0.594			
	All Lake Superior strains	3	3.0	0.57	0.56	0.623			
Sfo-D75	All strains	24	14.2	NC	NC	NC	0.030	-0.016	0.015
	Isle Royale	15	13.9	0.87	0.92	0.674			
	Apostle Island	14	13.2	0.87	0.89	0.988			
	Marquette	14	12.8	0.85	0.87	0.094			
	Traverse Island	12	12.0	0.88	0.90	0.003			
	Green Lake	11	10.1	0.81	0.86	0.053			
	Lewis Lake	11	10.9	0.83	0.83	0.101			
	Seneca Lake	14	13.9	0.88	0.79	0.006			
	All Lake Superior strains	19	14.0	0.88	0.90	0.498			
			Fixation indices over all loci				0.048	-0.030	0.019
			(95% bootstrap confidence limits)				(0.033 – 0.065)	(-0.053 – -0.010)	(0.001 – 0.044)

1239

1240 Table B3. Pairwise mean genetic differentiation indices (F_{ST}) calculated from 10 microsatellite

1241 loci for the seven lake trout hatchery strains for which tissue samples were available.

Hatchery Strain	Isle Royale	Apostle Island	Marquette	Traverse Island	Green Lake	Lewis Lake
Apostle Island	0.0127*					
Marquette	0.0144*	0.0095*				
Traverse Island	0.0142*	0.0124*	0.0180*			
Green Lake	0.0329*	0.0389*	0.0201*	0.0546*		
Lewis Lake	0.0468*	0.0451*	0.0590*	0.0668*	0.0379*	
Seneca Lake	0.0859*	0.0619*	0.0822*	0.0794*	0.0879*	0.0901*

1242 *significantly different from 0 at alpha = 0.05/21 = 0.002381

1243

1244

1245

1246

Appendix C – MCMC Traceplots from Saginaw Bay Walleye and northern Lake Michigan Lake Trout Applications

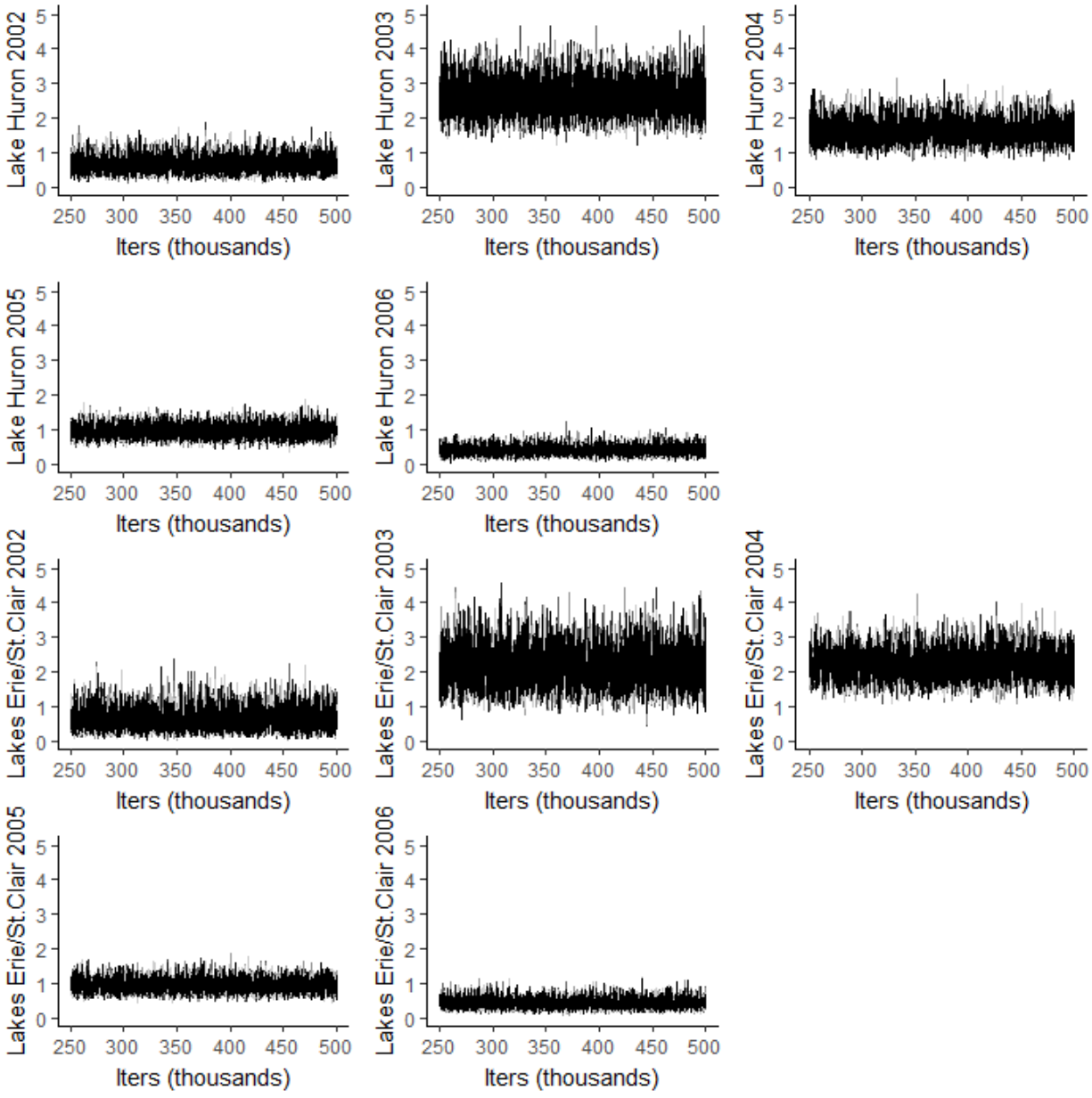

Fig. C1. Overlain traceplots for relative recruitments from Lake Huron and Lakes Erie/St. Clair for the 2002 to 2006 year classes for the five MCMC chains that were simulated for the Saginaw Bay, Lake Huron walleye application of the proposed estimation approach for indexing recruitment fluctuations in populations contributing to mixtures.

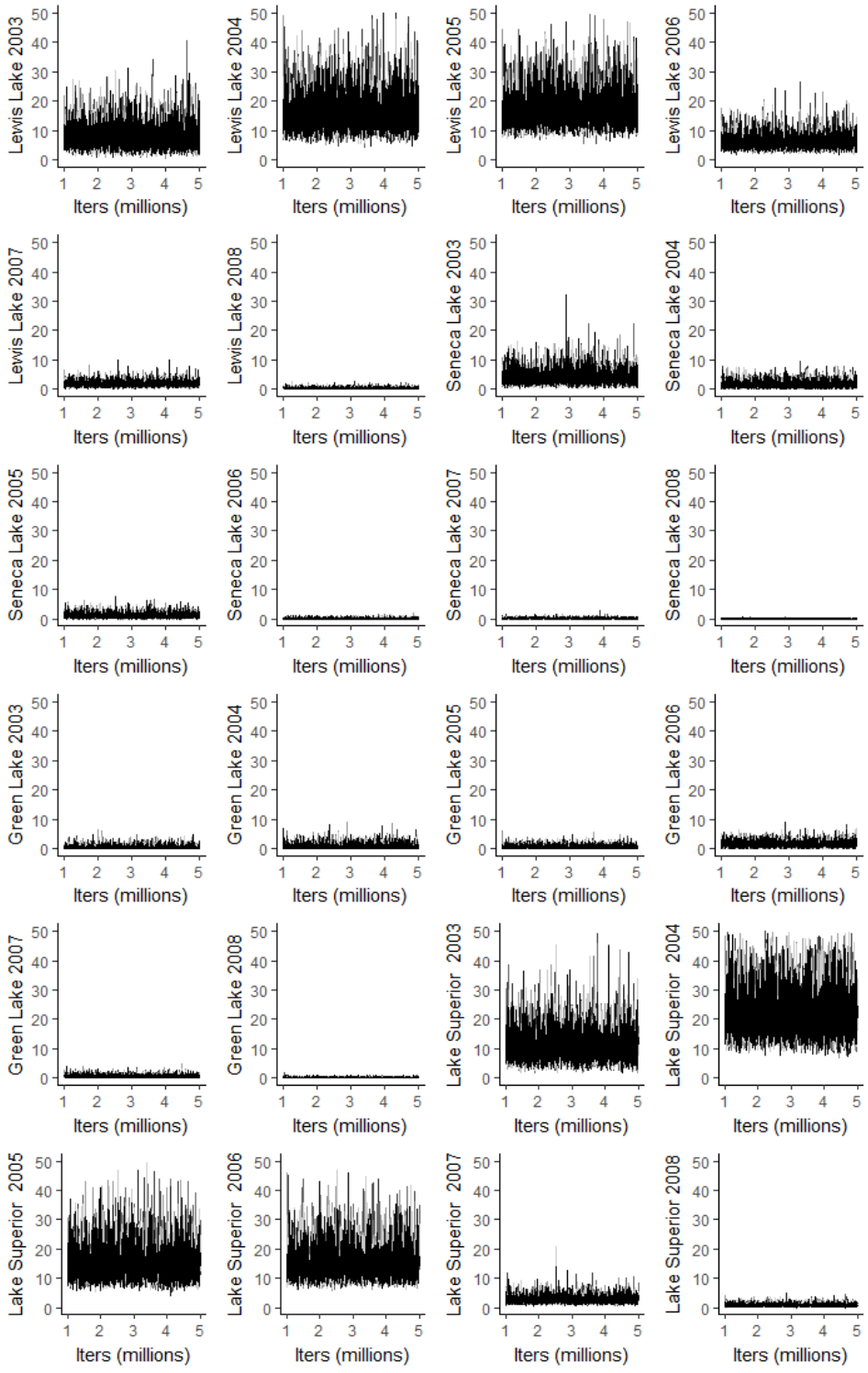

Fig. C2. Overlain traceplots for relative recruitments for Lewis Lake, Seneca Lake, Green Lake, and Lake Superior hatchery strains for the 2003 to 2008 year classes for the five MCMC chains that were simulated for the northern Lake Michigan lake trout application of the proposed estimation approach for indexing recruitment fluctuations in populations contributing to mixtures.